Available online at www.sciencedirect.com

ScienceDirect

Advances in Space Research 68 (2021) 85–104

ADVANCES IN SPACE RESEARCH
(a COSPAR publication)

www.elsevier.com/locate/asr

A cosmic dust detection suite for the deep space Gateway

P.J. Wozniakiewicz [a], J. Bridges [b], M.J. Burchell [a,*], W. Carey [c], J. Carpenter [c], V. Della Corte [d], A. Dignam [a], M.J. Genge [e], L. Hicks [b], M. Hilchenbach [f], J. Hillier [g], A.T. Kearsley [a], H. Krüger [f], S. Merouane [f], E. Palomba [d], F. Postberg [g], J. Schmidt [h], R. Srama [i], M. Trieloff [j], M. van-Ginneken [a], V.J. Sterken [k]

[a] Centre for Planetary Science and Astronomy, School of Physical Sciences, Univ. Kent, Canterbury, Kent CT2 7NH, United Kingdom
[b] Space Research Centre, School of Physics and Astronomy, University of Leicester, LE1 7RH, United Kingdom
[c] ESTEC, Keplerlaan 1, PO Box 299, NL-2200 AG Noordwijk, the Netherlands
[d] Institute for Space Astrophysics and Planetology (IAPS), National Institute for AstroPhysics (INAF), via Fosso del Cavaliere 100, 00133 Roma, Italy
[e] Department of Earth Science and Engineering, Imperial College London, Royal School of Mines, Prince Consort Road, South Kensington, London SW7 2BP, United Kingdom
[f] Max-Planck-Institut für Sonnensystemforschung, Justus-von-Liebig-Weg 3, D-37077 Göttingen, Germany
[g] Institute of Geological Sciences, Freie Universität Berlin, Berlin, Germany
[h] University of Oulu, 90014 Oulu, P.O. Box 3000, Finland
[i] Universität Stuttgart, Institut für Raumfahrtsysteme Raumfahrtzentrum Baden Württemberg, Pfaffenwaldring 29, 70569 Stuttgart, Germany
[j] Klaus-Tschira-Labor für Kosmochemie, Institut für Geowissenschaften der Universität Heidelberg, 69120 Heidelberg, Germany
[k] ETH Zürich, Institute for Particle Physics and Astrophysics, Wolfgang-Paulistrasse-27, CH-8093 Zurich, Switzerland

Received 2 October 2020; received in revised form 30 March 2021; accepted 2 April 2021
Available online 20 April 2021

Abstract

The decade of the 2020s promises to be when humanity returns to space beyond Earth orbit, with several nations trying to place astronauts on the Moon, before going further into deep space. As part of such a programme, NASA and partner organisations, propose to build a Deep Space Gateway in lunar orbit by the mid-2020s. This would be visited regularly and offer a platform for science as well as for human activity. Payloads that can be mounted externally on the Gateway offer the chance to, amongst other scientific goals, monitor and observe the dust flux in the vicinity of the Moon. This paper looks at relevant technologies to measure dust which will impact the exposed surface at high speed. Flux estimates and a model payload of detectors are described. It is predicted that the flux is sufficient to permit studies of cometary vs. asteroidal dust and their composition, and to sample interstellar dust streams. This may also be the last opportunity to measure the natural dust flux near the Moon before the current, relatively pristine environment, is contaminated by debris, as humanity's interest in the Moon generates increased activity in that vicinity in coming decades.
© 2021 COSPAR. Published by Elsevier B.V. This is an open access article under the CC BY-NC-ND license (http://creativecommons.org/licenses/by-nc-nd/4.0/).

Keywords: Cosmic dust; Moon; Impacts

1. Introduction

The flux of Solar System dust has long been of scientific interest (e.g. Schmidt, 1965; Brownlee, 1985; Grün et al., 2001; 2019). The dust (whose size typically ranges from the sub-micron to the mm scale) has several sources. Interplanetary dust predominantly originates from comets or asteroids, being dragged from cometary surfaces with subliming volatiles when they are nearer the Sun, or liberated from the surfaces of asteroids during impact events. There are also dust streams from planets like Jupiter, where dust can originate from the satellites (e.g. Io) and, once charged,

* Corresponding author.
E-mail address: M.J.Burchell@kent.ac.uk (M.J. Burchell).

https://doi.org/10.1016/j.asr.2021.04.002
0273-1177/© 2021 COSPAR. Published by Elsevier B.V.
This is an open access article under the CC BY-NC-ND license (http://creativecommons.org/licenses/by-nc-nd/4.0/).

be accelerated in the planet's electric and magnetic fields and emerge into interplanetary space as a dust stream (Grün et al., 1993). Even interstellar dust is observed inside the Solar System (Grün et al., 1993; Westphal et al., 2014; Sterken et al., 2019). In addition, particularly in the vicinity of the Earth itself, there is debris which arises from human activity in space (see Wozniakiewicz and Burchell, 2019, for a recent review of the flux of natural dust vs. debris in Low Earth Orbit). Measuring, and differentiating between, these different types of dust is a major area of scientific enquiry.

It is no surprise therefore that dust detection instruments have flown on many space missions. Nor that when new missions are planned, dust detectors are often considered for the payload. They help characterise the space environment and can provide scientific data on the amount and composition of the various sources of the dust.

The Deep Space Gateway (DSG), a plan to place a space station near the Moon (e.g. Crusan et al., 2019), offers the possibility for long observation times for instrument packages at 1 AU. A dust detector payload package is a prime instrument for deployment on such a platform. Given the long heritage of dust detectors in space, there is minimal technological development needed. The location near the Moon also removes the contribution from debris from human activities in Low to Geostationary Earth Orbit. Indeed, it offers the chance to measure the dust flux in a region close to the Earth before there is significant human generated activity. Paradoxically of course, any instruments used will still have to be capable of recognising debris from natural dust, in order to demonstrate its absence. This last point is important, because if the lunar environment is industrialised in decades to come, any measurements made today will be the baseline against which all future dust fluxes near the moon will be compared.

The key topics that can be studied by a dedicated dust platform on the DSG are listed below (also see Table 1 for more details):

- contrasting the results at 1 AU in Low Earth Orbit (LEO) and Lunar orbit (and flagging the presence/absence of debris related to human activities), this is a prime goal and if not done now will never be achievable;
- separation of the asteroidal and cometary fluxes and their compositions, to give their relative contributions to the interplanetary dust population;
- measurement of the interstellar dust flux and its composition, of growing interest since the Stardust mission captured interstellar dust grains in the inner Solar system;
- analysis of the organic content of dust grains, often neglected as it is the more refractory mineral grains that are easier to capture/analyse, but of vital interest regarding organic input to bodies from space

In addition, important support science can also be conducted.

- contributing to simultaneous measurements of dust fluxes along with other spacecraft elsewhere in the Solar System, (e.g. the Destiny + mission to study Apollo asteroid 3200 Phaethon and the Europa Clipper mission to the Jovian moon Europa, will both carry dust detectors and the Gateway dust detectors can look for similar particles at 1 AU to those detected near sources such as asteroids and planetary satellites)
- map the sky for dynamical dust properties,
- and validation/improvement of existing dust flux models to reduce uncertainties, a vital on-going activity.

The dust properties that are required to be measured are shown in Fig. 1 and listed in Table 2. The questions that arise therefore, are: What is the expected dust flux? And what constitutes an appropriate suite of instruments to measure it? In this paper we examine these questions. We start by summarising key features of the DSG itself. The range of available dust detectors is then described. Estimates of the flux of dust near the Moon are presented. Finally some model payloads are described with their expected dust measurement rates based on the flux models.

2. Deep space gateway

The DSG is a proposal from an alliance of agencies, to place a habitable space station near the Moon (e.g. Crusan et al., 2019). The dates for construction and launch are still somewhat subject to change, but current plans suggest hardware would be launched to lunar orbit starting around 2022-2024. Construction would be an on-going activity lasting several years. The station would not be permanently inhabited, crews would visit on occasion for short durations. A variety of lunar orbits are possible and were con-

Table 1
Key science goals for a lunar orbiting dust detector.

Science Goals and Key Technologies					
Possible Sources	Lunar dust (ejected)	Lunar dust (levitated)	Interplanetary dust particle including dust streams (cometary and asteroidal)	Interstellar dust	Debris (local, visiting spacecraft, cube sats, etc.)
Technology and heritage	Passive solid surfaces or foils (already flown)	Active resistive grids, pvdf or pzt sensors (already flown)	Impact ionization detectors with mass spectroscopy capability (already flown)	Microbalances (already flown)	Aerogel collectors (already flown)

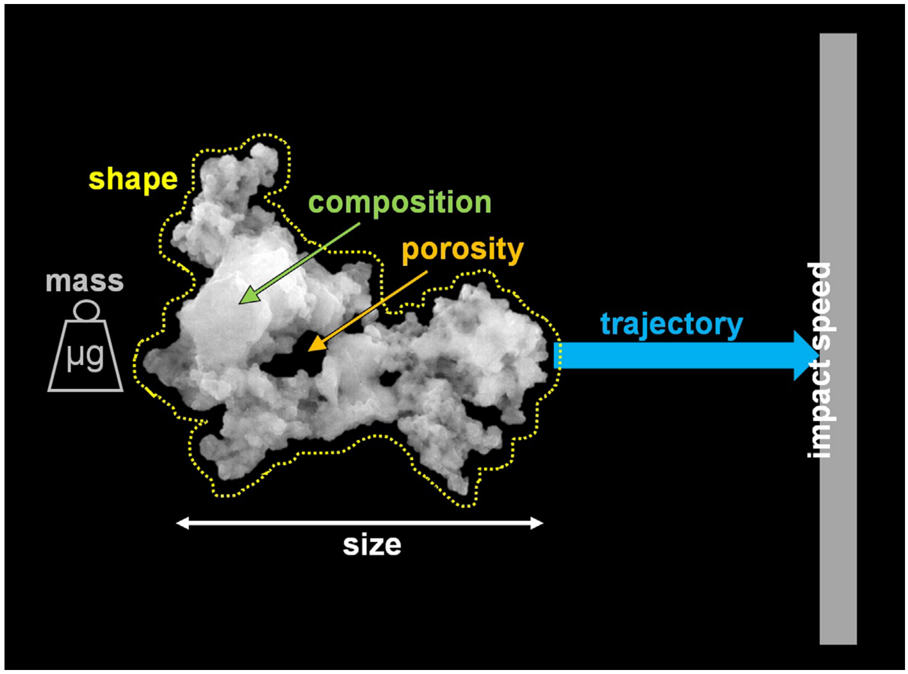

Fig. 1. Suite of properties of an impacting particle that need to be measured to fully characterise it. Combined with properties of all particles impacting a surface, these details enable the overall flux for the various populations to be determined. The central image is a SEM view of an interplanetary dust particle captured in the stratosphere. Source: https://apod.nasa.gov/apod/ap010813.html

sidered, but the favoured orbit is planned to be a near rectilinear halo orbit, with a fixed solar pointing direction, and a second fixed direction for the DSG which aligns with the lunar apex direction (e.g. Whitely and Martinez, 2016). Instruments can be hard mounted on the exterior of a module prior to launch, or have a soft launch (in a stowed environment) and then be deployed to their chosen location on the exterior of the DSG either robotically or, if astronauts are on board at the time, during extra-vehicular activities. Given that there will be occasional visits to the station, the possibility of retrieving instruments and returning them to Earth also exists.

3. Dust detectors

3.1. Overview

Even in the earliest days of spaceflight there were measurements of the dust flux in space (e.g. see Alexander et al., 1962, or Fechtig et al., 2001 for reviews). Since then there has been considerable development of technologies for dust collection in space (e.g. see Grün et al., 2001, and Auer, 2001) permitting in-situ measurements of dust in space (see for example "In-Situ Measurements of Cosmic Dust", Chapter 7 in Grün et al., 2001). The properties the detectors have to be able to measure should be sufficient to characterise the nature and origin of the impactor. A typical set of properties are shown in Fig. 1. However, there is no one detector type that can cover a full range of dust sizes (10 s of nm to mm scale) or impact speeds (m s^{-1} to more than 50 km s^{-1}). For example, impact ionisation-based active detectors are ideal for detecting particles below a few μm in size (they can in principle also detect larger grains, but charge saturation effects combined with small active areas and low fluxes at large sizes limit this), whilst impacting particles must be at least a few tens of μm in size to register on a resistive grid-based active collector. Active detectors provide real-time data for transmission home that can be linked to spacecraft attitude and thus provide details of original impactor trajectory, ultimately providing orbital information and the potential to link an impactor to a parent body.

Active detectors do not however always give accurate results. Early microphone type detectors for example, significantly over-predicted the dust flux (leading to fears of a major hazard to space vehicles in Earth orbit). This was later found to be due to their unforeseen sensitivity to thermal gradients in the crystals used in the microphones, interaction with high energy ions etc. (see Fechtig et al., 2001). A later example of uncertainty in reported fluxes arose with the Stardust mission to comet 81P Wild-2. Two instruments recorded the impact flux in real-time as the spacecraft flew past the comet. The Comet and Interstellar Dust Analyzer (CIDA) (Kissel et al., 2004) and the Dust Flux Monitor Instrument (DFMI) (Tuzzolino et al., 2004). Despite both instruments having flight heritage, their estimates of the flux for large (15+ μm) particles captured by the aerogel in the spacecraft differed significantly from each other: CIDA predicted very few such particles, and DFMI predicted 2800 ± 500. After its return, the Stardust aerogel was found to contain only a few hundred such particles (Hörz et al., 2006; Burchell et al., 2008b), compatible with neither of the predictions of CIDA and DFMI. This emphasises the importance of having a combined active and passive set of detectors.

Originally conceived as a way to measure flux, active detectors can also measure composition in some cases, e.g. if the particle is vaporised and the resulting plasma analysed. In comparison, passive detectors offer the simplest means of capturing dust, with analysis of impact features and interpretations of impactor characteristics (predominantly size and composition) being performed upon their return to Earth. For available passive detectors, collected samples can range from intact particles, through to heavily shocked and melted samples whose internal structure has been lost, but whose overall composition can still be measured. There are a wide range of possible analytical techniques available to study such small returned samples (e.g. see Zolensky et al., 2000; Stansbery and Draper, 2014). Furthermore, as long as the samples are not destroyed by any particular analysis method or some are simply placed into storage after retrieval, they can be subject to any future analysis techniques not yet even defined when the mission occurs.

It is also possible to combine passive and active technologies to leverage up the benefits of each. In the rest of this section, the various main types of instruments are described. It is assumed that collection will be at high-speed, limiting the detector technologies.

3.2. Passive detectors: exposed surfaces

The simplest dust collection method deployed in space is to expose a surface and retrieve it. Depending on the relative orbits of the collector and the dust particle, the impact speed in LEO orbit for example would typically be 7–11 km s^{-1} for debris particles and 15–20 km s^{-1} for natural dust. At the Moon, the impact speed for interplanetary particles would be similar (minus any terrestrial gravitational effect). At such speeds, the resultant impacts are termed hypervelocity. That is, the speed of the resultant compression waves in both the target and impactor is less than the speed of the impact. The result is that a shock wave traverses the materials involved, with the material in front of the shock being unaltered, whilst that behind it is shocked to, and then released from, a state of extreme compression, involving high pressures in the many 10 s to 100 s of GPa range. Given that this is in excess of material strengths (typically 10–100 s of MPa) the materials behave as if they had no shear strength and flow in a hydrodynamic fashion. Release from this shock state heats the materials sufficiently that they may melt or be vaporised. The result is the formation of a crater, which in a ductile material will have a bowl shape surrounded by a raised rim wall, and whose interior will be lined with melted projectile residue (see Fig. 2). An example of the use of exposed surfaces in space was the NASA Long Duration Exposure Facility (LDEF), which was placed in Low Earth Orbit for 5 years and 7 months in 1984 and retrieved in 1990 (e.g. Mandeville, 1991; Murr and Kinard, 1993). LDEF was intended to monitor the effects of the space environment on a variety of materials and thus included a variety of passive experiments dedicated to providing data on dust particle composition and flux, for example the Chemistry of Micrometeoroids Experiment (A0187-1) and Space Debris Impact Experiment (S0001) (e.g. Mandeville and Borg, 1993; Hörz et al., 1993; Humes, 1993). Non-dedicated metal surfaces on board LDEF also provided important data – for example, many impact features and associated residues were analysed from experiment tray clamps (Bernhard and Zolensky, 1993). A review of these surfaces and studies can be found in Ortner and Stadermann, 2009.

Most (large) surfaces specifically used as passive detectors are metals, usually of high purity. However, strictly speaking, all that is ideally required is the combination of a large exposed area and a long exposure time. This maximises the number of impacts. Solar panels are thus ideal surfaces for accumulating impact features, even though their front surface is a brittle material (glass) and their interior structure and rear surfaces are complex with many elements present. The brittle nature of the glass means the crater that was initially formed is then surrounded by a larger spallation zone where lightly shocked material has been lifted away late in the crater formation process (Fig. 3). Impacts can also occur on the rear of the panels, but unless large, tend to be harder to identify. Examples of retrieved solar panels include those of the EuReCa satellite after an 11 month exposure in Low Earth Orbit (Drolshagen et al., 1995) and those of the Hubble Space Telescope (HST), where panels were retrieved twice by service missions after 3.6 years on orbit (Drolshagen et al., 1997) and 8.25 years in orbit (Kearsley et al., 2005a). However, as stated, solar panels are multi-layered structures with a complex composition. This makes the identification of the impactor material difficult, as it may not be clear which elements come from the impactor and which from the solar panel (e.g. Kearsley et al., 2005a). This is a particularly acute issue when trying to identify which impactors have an origin in human activity in space, i.e. are debris, and which may contain several of the same marker elements as do the solar panels. Nevertheless, as indicated, solar panels have been retrieved from space and used in determining both the flux and composition of cosmic dust.

After retrieval from space, (in the past via the space shuttle for example), the exposed surfaces of whatever type, are typically surveyed with high resolution photography and microscopy to locate and measure the larger features. Smaller areas are then scanned in scanning electron microscopes (SEM) to measure features at sizes less than say a few tens of µm (e.g. see Price et al., 2010). Such measurements provide the basic information needed to obtain a flux estimate. To do this, the observed size of the craters (e.g. Love et al., 1995) has to be combined with a calibration that relates impact feature size and shape to impactor properties (e.g. Burchell and Mackay, 1998, McDonnell

Table 2
Science goals mapped onto detector abilities.

Science Objective	Measurement requirement	In-situ measurement instrument	Sample return measurement instrument
Particle elemental composition	Mass spectra capable of resolving 1 amu, in both anions and cations	Impact ionization spectrometer	Aerogel Foil capture system
Particle Mass	Down to ng	Impact ionization spectrometer	
	50 μm to 1 mm	Multi-layer resistive grids	Multi-layer resistive grids
Particle Size	50 μm to 1 mm	Multi-layer resistive grids	Multi-layer resistive grids
	1 μm to 1 mm	Vibration sensor mounted on baseplate of detectors	Aerogel Foil capture system
	1 μm to 100 μm	Pick-up charge grids	
	Sub-micron	Impact ionisation by TOF spectrum	Aerogel
	Nano-dust	Impact ionisation by TOF spectrum	
Particle bulk density	To within few hundred kg m^{-3}	Multi-layer resistive grids	Multi-layer resistive grids
	To within few kg m^{-3}		Aerogel
Particle porosity	Meso-porosity		Foil capture system
	Micro-porosity		Aerogel
Particle trajectory	Direction to ± 5°	Impact ionization spectrometer with pick-up electrodes for induced charge	Aerogel
	Speed to few %	Impact ionization spectrometer Foil telescope with multiple layers and vibration sensors	
Particle compositional structure	Detailed mineralogy and crystallinity		Aerogel Foil capture system

and Gardner, 1998). These calibrations are commonly derived from data provided by laboratory simulations. Use of these calibrations has an uncertainty, however, in that in the subsequent analysis of real data, the mean impact speed of a population is used to assess each impact rather than the (unknown) actual speed of an individual impact. Further, the composition (often bulk density) and internal structure (e.g. porous or compact) of a particle can also play a major role in defining the size and shape of the resultant crater (e.g. Kearsley et al., 2008). The angle of impact can also be influential, as can the general shape of the impactor (e.g. Burchell and Mackay, 1998). Nevertheless, averaging over all these variables does permit a flux estimate.

The composition of impactors can be found, for example, from SEM-EDX analysis, where emission of characteristic energies from the various elements in the impact residue can be stimulated (e.g. on metals see Kearsley et al., 2007a, and on glass see Kearsley et al., 2007b). Further, focussed ion beam sections of impact residue can be extracted from craters and studied by TEM, and crystallinity determined (if any). Raman spectroscopy has also been shown to be effective on residues from mineral samples fired into metals at speeds of up to 6 km s^{-1} (Burchell et al., 2008a). This suggests that melting of the projectile is incomplete at such speeds, and it has been shown that the crystallinity observed in such crater residues is that of the original impactor and not the result of re-crystallisation of the melt (Wozniakiewicz et al., 2012a). Even at high mean impact speeds, e.g. interplanetary dust impacting LDEF, or the TiCCE experiment in LEO on the EuReCa spacecraft (Yano et al., 1996), the impact craters often still provide residue analysable with SEM-EDX. However, some elements are more volatile than others, so the absolute ratios of elements measured in impact residues is not automatically the same as the ratios present in the pre-impact particle (e.g. Lange et al., 1986). In addition, melting of both impactor and collector surface can result in residues that display a mixture of their chemistries (e.g. Wozniakiewicz et al., 2012b).

3.3. Passive detectors: Thin foils

A variation of dust capture on relatively thick (i.e. semi-infinite) targets, is the use of thin foil detectors. Here, the impactor punches a hole in the thin foil. A conversion from the observed hole size is then required to obtain the impactor size (e.g. Gardner et al., 1997). However, for very high speed impactors, on foils whose thickness is less than the impactor size, the hole size conveniently converges towards the particle size. The rim of the hole can also be examined with SEM-EDX to look for traces of the impactor to determine its surface composition. Once it has passed through the thin foil, the projectile may continue roughly intact, or, may have been disrupted. The fragmented projectile material will then continue in a roughly forward direction, spreading out as it does so, making its capture on a subsequent foil layer or a thicker base plate easier (much like the principle of a Whipple shield). In this fashion a multi-layer foil detector can be constructed, which provides particle size and trajectory, along with composition (e.g. Fig. 4).

An early example of a multilayer foil dust detector deployed in space, was the microabrasion foil experiment (MFE), carried on the space shuttle mission STS-3 in 1984 (McDonnell et al., 1984). Being a STS flight, the expose time was only eight days in Low Earth Orbit, but

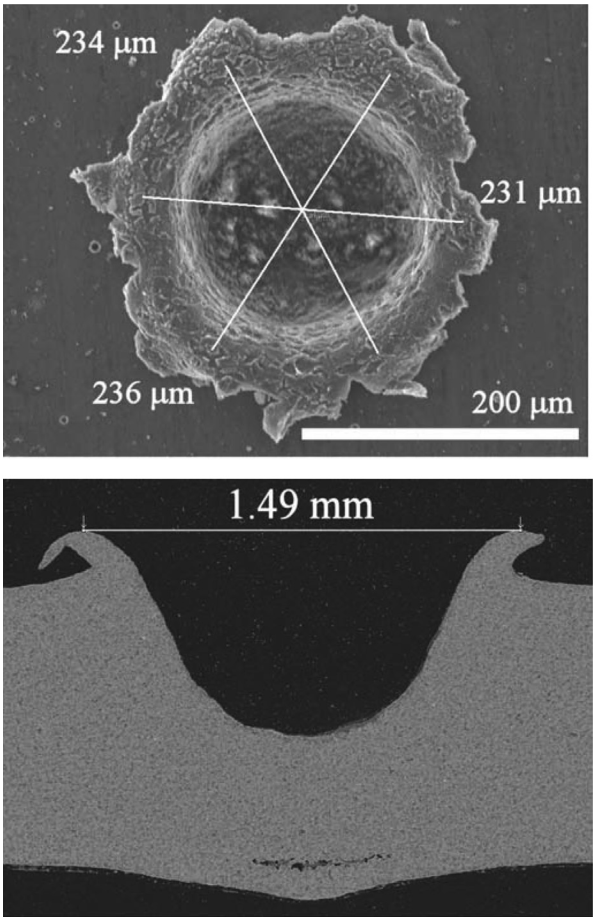

Fig. 2. Bowl shaped crater in metal. (a) Impact of an enstatite grain on aluminium foil in the laboratory at 6 km s^{-1} (top view). (b) A section through a crater on aluminium at 6 km s^{-1} (side view). Source: Figs. 8 and 10, Kearsley et al. 2006.

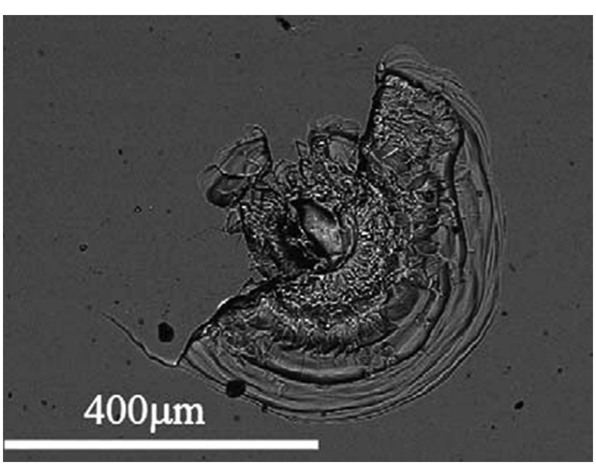

Fig. 3. Impact crater in glass solar cell from the HST. There is a deep central pit, partly surrounded by a shallower and, in this example, asymmetric spall region. Source: Fig. 7, Kearsley et al., 2005.

four hypervelocity impact features were identified in the analysis after the return to Earth. With the concept having been demonstrated, foil detectors were then carried on LDEF (e.g. see McDonnell and Stevenson, 1991 and other

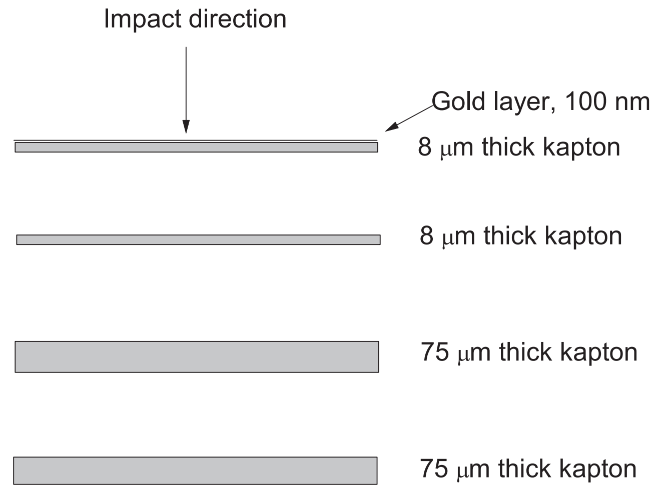

Fig. 4. Schematic of a multi-layer foil dust telescope (not to scale). The thickness of the lower layers is greater than the upper layers, to help capture larger particles and can be varied based on flux models. The presence of a gold layer on the uppermost surface is partly for thermal control and partly to enable easy identification of impact features in subsequent analysis.

papers in the same volume). Since then, several more such experiments have flown (e.g. TiCCE on EuReCa in the early 1990s, see Gardner et al., 1996), and a new generation of multi-layered foil collector have been designed and tested in the laboratory (e.g. MULPEX see Kearsley et al., 2005b, and ODIE see Wozniakiewicz et al., 2019). In such detectors, designed specifically for deployment in LEO, the top foil needs to be coated to prevent damage by atomic oxygen erosion (in Low Earth Orbit). For a detector near the Moon, coating of the foils is still required, not to prevent erosion, but to allow ready subsequent detection of the penetration holes and impact craters in, for example, a SEM; gold or palladium coatings are considered particularly suitable for this purpose since they provide a high contrast (high atomic number) background in backscatter electron images against which dark impact features/penetration holes can be easily located (Kearsley et al., 2005b).

Thin foil detectors can be thus seen to have a long heritage of space use. They are low mass and relatively robust to use. Analyses of LEO exposed MLI and studies of polymer foils impacted in the laboratory at hypervelocities have demonstrated the ability of such foils to capture and retain substantial quantities of easily identifiable residue (e.g. Graham et al., 2003; Kearsley and Graham, 2004). In laboratory studies, multi-foil detectors have been shown capable of providing particle sizes and preserving details of chemistry for particles ranging in size from micron to mm scales (Kearsley et al., 2005b, 2005c).

3.4. Passive detectors: aerogel

Although very high speed impacts on dense surfaces result in extreme shocks (altering the impactor), the process is different if the same impact occurs on an underdense target. Such underdense materials have a high degree of microporosity, so their bulk density is not that of the material the target is made of, but has to include the contribution of the void space as well. Impacts into such materials result in much lower shock pressures, and can result in tracks in the target. A typical example of such material is silica aerogel (e.g. Bunch et al., 1991; Barrett et al., 1992; Kitazawa et al., 1999; and see Burchell et al., 2006a for a review of the use of aerogel to collect dust in space). As well as capturing dust grains relatively intact, the track in the aerogel is also aligned with the impact direction, permitting discrimination between different sources of dust if the pointing history of the spacecraft is known at the time of impact (e.g. Burchell et al., 1999a; 2012). The shock pressures for particles impacting low density (25 kg m^{-3}) aerogel have been estimated to be less than a GPa, even in impacts at 6 km s^{-1} (Trigo-Rodríguez et al., 2008). Well condensed mineral or metallic impactors will tunnel into aerogel, with a significant portion of the grain found intact near the end of the aerogel track (Fig. 5a).

For well consolidated grains with high melting points, capture in aerogel works well at speeds up to around 10 km s^{-1}, (e.g. see Burchell et al., 2001; 2009a, who show minimal loss of projectile mass for glass beads of 12 to 106 μm diameter impacting aerogels of a range of densities

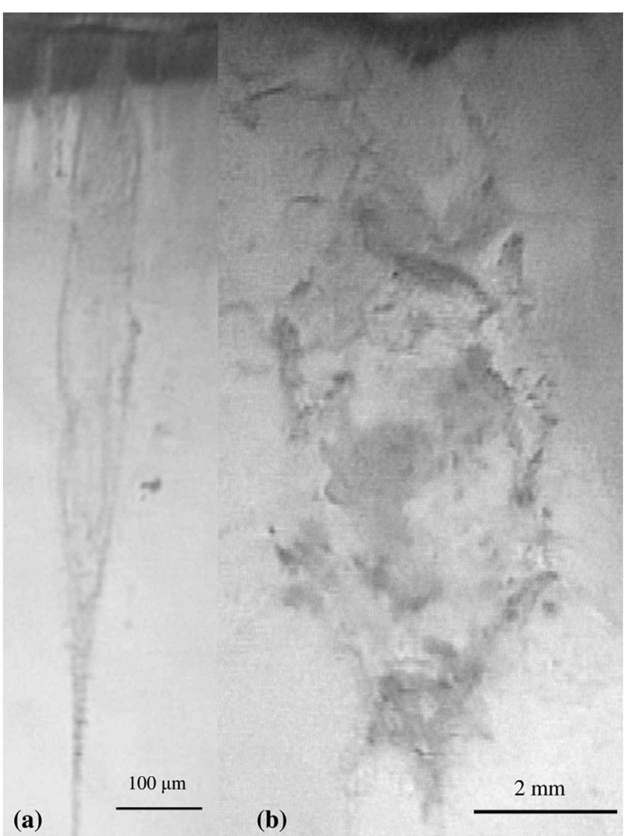

Fig. 5. Aerogel tracks (a) Carrot track, (b) Bulbous track. In both cases a side view is shown, with the impact coming from the top. Source: Fig. 5 Burchell et al., 2008b

at speeds from 1 to 6 km s^{-1}). However, small impactors, particularly of low melting point can undergo significant mass loss during capture. For example, it has been shown that in aerogel of density 25–35 kg m^{-3}, 20 μm diameter polystyrene projectiles were reduced in diameter by ~50% and lost some 84% of their mass during capture at 6 km s^{-1} (Burchell et al., 2009b). There is also evidence that at impact speeds of 15 km s^{-1}, small (sub-micron sized) non-refractory impactors no longer produce significant captured material in the track in the aerogel, and above 20 km s^{-1} small mineral grains can also fail to produce macroscopic fragments in the resultant aerogel track (Postberg et al., 2014). Analysis of particles captured in aerogel thus has to focus not only on macroscopic intact fragments, but also on what may have been infused into the aerogel along the walls of a track (e.g. Ishii et al., 2008a; 2008b).

A variety of aerogels can be manufactured, including alumina (Li et al., 2017), titanium (Ayers and Hunt, 1998) and zirconium (Liu et al., 2018), and examples of their use to capture particles in laboratory tests include Jones and Flynn (2011). However, most aerogel used to date in space is silica aerogel. Since silica aerogel is transparent, dust grains captured in it can be measured in situ in the aerogel, i.e. size can be determined optically and composition by Raman spectroscopy (e.g. see Burchell et al., 2001; 2004; 2006b). Equally, grains can be extracted (e.g. Westphal et al., 2004) and made available for any laboratory analysis technique that can handle micron sized particles (see Zolensky et al., 2000; Stansbery and Draper, 2014). For example, early studies on laboratory samples fired into aerogel using X-ray microprobes include Flynn et al., 1996 and Westphal et al., 1998. Examples of synchrotron beams used in the analysis of returned samples to aid in their characterisation include Noguchi et al., 2007; Nakamura et al., 2008a; Bridges et al., 2010; Flynn et al., 2014; Hicks et al., 2017.

Several experiments have deployed aerogel in space. Early ones included flights on the STS in the 1980s (Maag and Linder, 1992), then on the EuReCa satellite in the 1990s (e.g. Brownlee et al., 1994; Burchell et al., 1999a), on the outside of space stations such as Mir (Shrine et al., 1997; Hörz et al., 2000) and the ISS (e.g. such as on the MPAC experiment exposed to 3 years starting in 2001, Neish et al., 2005, and the MEDET experiment exposed for 18 months starting in 2008, Woignier et al., 2013). A recent use of aerogel to capture dust in space was the Japanese Tanpopo experiment on the exterior of the ISS (Tabata et al., 2014); this exposed panels of aerogel for 3 years on the exterior of the ISS from 2015 to 2018 and panels were replaced on an annual basis during this time.

However, perhaps the best known example of dust collected in space in aerogel is the NASA Stardust mission, which collected freshly emitted cometary dust during a flyby of comet 81P/Wild-2 at 6.1 km s^{-1} (e.g. Tsou et al., 2003; Brownlee et al., 2006; Hörz et al., 2006; Brownlee, 2014). Cometary dust particle sizes measured in Stardust were estimated to include grains up to 10 or 15 μm diameter. About 2/3rds of cometary dust grains captured by Stardust produced tracks as per Fig. 5a (see Burchell et al., 2008b) containing a compact, well-preserved terminal particle. However, even shock pressures just below 1 GPa can cause weak, friable cosmic dust particles to break apart, but their components are then captured in the walls of the bulbous cavity that opens in the aerogel or in short tracks beneath the cavity (Fig. 5b); about 1/3rd of Stardust cometary dust tracks were of this type. Around 2% of Stardust cometary dust tracks were a variation of the bulbous type, with no large sub-grains surviving in small tracks radiating from the main cavity. Through these analyses, Stardust provided a unique insight into cometary formation. Unexpected findings have to date included the relatively high abundance of refractory melt inclusion fragments (chondrules and CAIs) and evidence for aqueous alteration on the parent body (Brownlee et al., 2006; Nakamura et al., 2008b; Simon et al., 2008; Westphal et al., 2009; Bridges et al., 2012; Joswiak et al., 2014; Hicks et al., 2017).

Stardust also deployed aerogel to capture interstellar dust grains in the inner Solar System. This was achieved by exposing aerogel samples into the expected direction of interstellar dust, and using the pointing history of the resultant tracks to identify the likely origin. The result was that, at <1.5 AU with an exposure time of 195 days, analysis of aerogel with a surface area of 250 cm^2 yielded 3 putative interstellar dust grains, all just over 1 μm (3 pg) in size and yet still detectable on the aerogel (Westphal et al., 2014). A further 4 candidate interstellar grains were found in the same collector in an analysis of 5 cm^2 of exposed aluminium foil. The contrast in the measured rate per unit area of found particles illustrates that it is relatively more difficult to find small particles in aerogel. However the different capture mechanisms permit a more complete picture of the original grains to be obtained when combining results from foils and aerogel.

3.5. Active detectors: vibration sensors

Active detectors are ones which provide a real-time readout of their data. A simple such design is to have a surface on which are mounted vibration sensors, e.g. lead zirconate titanate (PZT) crystals (e.g. Tuzzolino et al., 2003 or Nogami et al, 2010), or polyvinylidene fluoride (PVDF) films (e.g. Burchell et al., 2011; Piquette et al., 2020). If the surface is uniform in its transmission properties, then timing data from each of the (minimum) three sensors would permit triangulation of the impact point. Once the distance to each sensor is known, any transmission loss can be adjusted for, and the amplitudes of the signals used to estimate how much energy or momentum was transferred to the target during the impact. If a calibration is known, this can be used to provide an estimate of the incident energy or momentum. Problems can arise from false signals due to noise, spacecraft vibration etc., so to overcome this, rigorous testing of the detector in simulated space exposure conditions is required, combined with care taken during analysis.

Surfaces used for other purposes, such as a solar sail, can be equipped with PVDF sensors and used as large area detectors. An example of this is the ALADDIN dust detection experiment on the IKAROS spacecraft (Hirai et al., 2014). Another example, is the addition of PVDF sensors to multi-layer thermal insulation to act as a dust impact detector (e.g. Ikari et al., 2019). The future JAXA Martian Moons Exploration mission is planned to feature a 1 m^2 dust detector (CMDM) which will use impacts on a thin film (the front layer of multi-layer insulation) equipped with pzt sensors to detect particles above 10 μm in size (Kobayashi et al., 2018).

If several thin layers are used as the target surfaces, and they are arranged one above the other, then the trajectory and speed of the transiting particle can be found (assuming no loss of speed during passage through the thin target layer). Provided the space pointing direction of the sensor system is known, this then permits orbit identification. In addition, knowledge of the particle speed, combined with the estimate of the energy or momentum, would permit an estimate of particle mass.

It is also possible to use PVDF films as impact sensors themselves, rather than as vibration detectors. Examples of this include the high rate detectors on the Cassini (Tuzzolino, 1995) and Stardust missions (Tuzzolino et al., 2003), and the Student Dust Counter on the New Horizons mission (Piquette et al., 2019). These detectors usually have small active areas and operate on a volume depolarisation occurring when a small dust grain hits. The resulting change in capacitance can be measured and related to the impactor.

3.6. Active detectors: resistive grid

Several versions of resistive grid detectors exist. The general idea behind these is to lay down a resistive grid of, say, parallel copper lines on a substrate. Example substrates include circuit boards (Burchell et al., 2013; Faure et al., 2013) or thin films (Nakamura et al., 2015). If the lines are of narrow width and close together, then an impact will break a line (or several lines) and change the resistance of the grid. If the resistance of each line is monitored, a step change in resistance will indicate a break, implying an impact. Equally, the total resistance can be read out, and again a change will indicate how many lines have been broken in the impact event. In such methods, only the lateral spread of the damage across the resistive tracks is measured, but if it is assumed the damage is circular, the size of the impact feature can be found to an accuracy depending on the line width and spacing (a calibration is then needed to relate this to the impactor size). A detector based on the design of Faure et al. (2013) was flown on the Japanese nanosatellite Horyu-II in 2012.

3.7. Active detectors: light curtains

If a beam of light is focussed onto a light detector, and the beam is interrupted by the passage of a particle, the output of the light detector will be interrupted. An array of such light beams can be built which effectively forms a thin plane of neighbouring parallel beams. If a second plane were placed just behind the first one, but rotated by 90°, a near x, y, z coordinate can be obtained for the particle, along with timing information. An array of such pairs would yield the trajectory and speed of the particle. A variation on this (named Giada) was flown on the Rosetta mission to comet 67P/Churyumov–Gerasimenko (e.g. Della Corte et al., 2015, 2019). This had only one plane of light beams per layer and two layers in total, but did provide an estimate of the dust flux near the comet. However, due to design limitations, this technology currently only works well for particle speeds of up to a few hundred m s^{-1}, well below what is required for dust detection at the DSG.

3.8. Active detectors: charge sensor grids

Particles in space are charged via a variety of mechanisms such as the photoelectric effect, solar wind etc. (see Whipple, 1981, for a review). The nature of the particle is also important, e.g. composition and size. The result can be a charge that is +ve or –ve and the voltage can be as much as 10 V in interplanetary space corresponding to charges in the fC range. Various detectors were flown on spacecraft missions to measure charge on dust particles (e.g. Helios, Galileo, Ulysses and Cassini, see Auer, 2001 for a review). Passage of a charged particle near a conduction wire, will induce a pulse in the wire, which can be used to flag the passage of the particle. If a plane-like arrangement of such wires were built, and several pairs of such arrays used, similar to the case for obtaining individual x, y, z coordinates with light curtains (see above), then particle charge, speed and trajectory can be obtained (e.g. Auer, 1995; Kempf et al., 2004).

3.9. Active detectors: microbalance

Microbalances are sensitive piezo-electric devices whose frequency of oscillation changes when a mass is placed on its surface (see Sauerbrey, 1959; Zhang et al., 1997). These can be sensitive enough to detect individual masses down to micron size (e.g. Palomba et al., 2002). The impact speed of the dust has to be low enough to allow it to adhere to the surface and not rebound (Palomba et al., 2001). Regarding the study of dust particles in space, the devices are thus best suited to accumulation of low speed dust and as such have been of interest when monitoring of contamination by, for example, thruster firings (Dirri et al., 2019). Modern space qualified microbalances are available commercially e.g. by QCM Research Company, CrystalTeck Corp and MEISEI Electric Co. A typical instrument would have a volume of $(5 \times 5 \times 5)$ cm, with a 0.28 cm^2 active surface area and a power consumption of less than 1.5 W. These can be part of a payload on a spacecraft to monitor the general space environment, or be sub-components of larger dust detectors, e.g. the Giada dust detector on the Rosetta mission (e.g. Della Corte et al., 2019). A review of the use of microbalances in space can be found in Dirri et al. (2019).

3.10. Active detectors: impact ionization detector

If a particle of a few microns or smaller, impacts a metal surface at a speed in excess of a few km s^{-1}, as already described, the result is usually a crater in the target, often lined with impact melt and residue. A fraction of the impactor (and target) is also often sufficiently heated to vaporise, and is energetic enough to produce a plasma. The charge produced can be collected by a grid mounted above the target (if a potential difference is applied between target and grid). The collected charge is proportional to $m^{\alpha}v^{\beta}$, where m is the mass of the impactor and v its speed. Usually, $\alpha = 1$ is assumed, and β found by laboratory experiments for different targets (e.g. see Dietzel et al., 1973; Dahlmann et al., 1977; Burchell et al., 1999b). It is also possible to separately determine v from the rise time of the signals, permitting an estimate of the impactor mass. Typical examples of space missions which carried impact ionisation detectors to measure dust fluxes, include the Ulysses spacecraft which measured dust fluxes at high ecliptic latitudes (Baguhl et al., 1995; Göller and Grün, 1989), as did the Galileo spacecraft which orbited Jupiter (e.g. Krüger et al., 2006), and the LADEE spacecraft which was in a low lunar orbit in 2013 (Horányi et al., 2015).

In the 1990s, the Cassini mission to Saturn was launched with an impact ionization detector (the Cosmic Dust Analyser, CDA) with a high electric field just above the target, followed by a lower field over a longer distance to focus the accelerated ions onto a detector (Srama et al., 2004). The result was a squat cylindrical (or barrel) shaped device with an open top and a curved base. The diameter was 41 cm. The target used was high purity rhodium with a diameter of 16 cm. A gold-coated impact ionisation target surrounded the rhodium target for ordinary impact ionisation detection of the particles to obtain their mass and velocity. The design permitted time of flight (TOF) mass spectra to be obtained from the ionic plasma arising from each impact on the rhodium target. The high electric field of the TOF target accelerated the ions, which then drifted to the detector. The resulting TOF mass spectra are not necessarily purely elemental. Depending on the energy density in the impact, molecular fragments are initially formed in the plasma, and only at high speeds (typically above 20 – 30 km s^{-1}) are purely elemental mass spectra usually.

This issue has been long known (see Hornung and Kissel, 1994, for a discussion and mathematical treatment of this question). At low impact speeds there is surface ionization, whereas at higher speeds there is complete volume ionisation. There are also velocity thresholds for partial or full ionization of different elemental species, and this is illustrated for example by Dahlmann et al., 1977, or Ratcliff et al., 1997a; 1997b. A step forward in understanding this was the wide-spread adoption of the use of non-metal projectiles in laboratory impact experiments (the particles are accelerated electrostatically, so are coated with thin overlayers of either metal or conducting polymers). This significantly improved the ability to systematically study how different minerals and organics ionise in impact events vs. impact speed (see for example Goldsworthy et al., 2002; 2003; 2012; 2014; 2018;; Burchell and Armes, 2011; Hillier et al., 2009; Fiege et al., 2014). The velocity thresholds depend on both the chemistry of the mineral and on how the impact energy is coupled into the impactor (i.e. are target dependent), so are not universal. Fiege et al., 2014 reported that at above 15 km s^{-1}, differentiation of mineral types is relatively straightforward. Similarly, Hillier et al., 2018, have shown that even at low speeds, some minerals are still ionised, e.g. Mg^{+} at less than 3 km s^{-1} and Si^{+} at between 6.9 and 9 km s^{-1}. Relative sensitivity factors also have to be taken into account when determining the impactor chemistry from the relative magnitudes of peaks in observed mass spectra. Based on regularities in the spectra, the underlying chemistry of organic compounds can be identified, for example aromatics yield differently spaced spectra to aliphatics and molecular fragments distinctive of specific compounds can be identified even at speeds below 10 km s^{-1} (e.g. see Goldsworthy et al., 2002; Burchell and Armes, 2011; Hillier et al., 2009; 2014;; Khawaja et al., 2019; Srama et al., 2009).

A second issue is whether the grains are single compositions or are assemblages of multiple smaller grains of differing compositions. Large grains are indeed often assemblages (e.g. see analysis of returned samples from Stardust for example, Hörz et al., 2006; Burchell et al, 2008b), whereas smaller grains <200 nm tend to be single compositions (e.g. Cohen et al., 2019). Large grains (above 10 s of micrometer scale) will saturate typical ionization detectors, so will not contribute significantly to the data set, whereas small grains dominate the size distribution so will also dominate the data. Where multi-component impactors are present, it is still possible to identify components by the presence of distinctive molecular species or elemental peaks in the spectra, combined with cluster analysis on large data sets (e.g. Cohen et al., 2019). To set a possible scale, we note that Wozniakiewicz et al. (2013), reported the mean sizes of silicates in four different CP IDPs ranged from 50 to 200 nm, and that the mean size of sulfides in the same four CP IDPs ranged from 40 to 100 nm. This suggests that in these cometary grains, a transition from single crystal to a more porous aggregate structure, and thus a transition from monomineralic to mixed minerals, occurs somewhere near 100 nm.

The mass resolution of the CDA instrument was typically m/Δm of 10–50 (Goldsworthy et al., 2003; Srama et al., 2004). Modern versions of such detectors can now achieve a higher resolution, with m/Δm between 100 and 150 planned for the Destiny + Dust Analyser (DDA) which aims to flyby the Apollo asteroid 3200 Phaethon at 0.87 AU (Masanori et al., 2018; Krüger et al., 2019). In addition, the Destiny + instrument should achieve a measurement of particle speed accurate to 10%, and trajectory to 10°. Plans for the next generation of these detectors include a rotating base and a Y (or U) shaped yoke, permitting pointing of the device in a wide range of directions. In the future, if approved for flight, detectors using an orbitrap arrangement to detect the ions will permit far higher mass resolutions in the tens of thousands or more (e.g. see Zubarev and Makarov, 2013, Briois et al., 2016).

3.11. Plasma detectors

There are instruments deployed in space which detect radio frequency (RF) signals. If a dust particle were to hit the spacecraft body nearby, the plasma generated by the impact can be detected if it couples to the RF antenna. This was shown by the Voyager 2 spacecraft near Saturn (Gurnett et al., 1983). This method of detection is still used and is discussed for example in Rudolph et al., 2014, Meyer-Vernet et al., 2017, Mann et al., 2019 and Vaverka et al., 2019. A known issue with plasma detectors is normally their calibration and the reliable identification of dust impacts.

3.12. Combined detectors

It is of course possible to combine different technologies into one dust detector. For example, the Cassini CDA detector had charge sensor grids above its impact ionization stage. This aids in particle speed measurement, and hence determination of particle mass. It also helps reduce ambiguities due to noise in one component being falsely identified as a real signal. More recently, the NASA Dragons detector (Liou et al., 2015; Doyle et al., 2016) combined resistive and acoustic grids in multiple layers. This was flown on the exterior of the ISS in 2018.

It is also possible to combine vibration sensors on thick baseplates behind resistive grids on thin foils; multiple layers giving extra or redundant information and helping remove false signals due to noise. Equally, a passive detector, such as aerogel or even just a polished thick metal plate, can be positioned behind thin films with vibration sensors, and after retrieval, the trajectory of a "hit" in the active component (which can be linked to impactor orbit if the spacecraft attitude is known) can be extrapolated to the appropriately located track in the aerogel or crater in the baseplate and thus linked to results from the in-depth analyses performed upon return to Earth. By combining these detector methods it becomes possible to provide a more complete picture of each individual impactor (e.g. impact speed, orbital information, composition, size etc.).

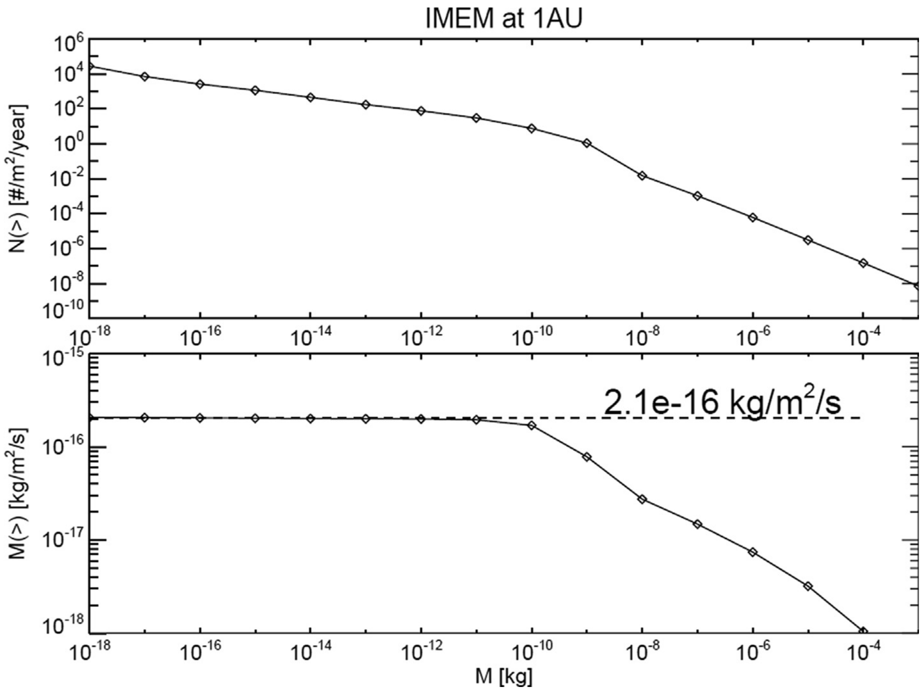

Fig. 6. Flux from the IMEM model (Dikarev et al, 2005). Upper panel: Cumulative number flux vs projectile mass. Lower panel: Cumulative mass flux vs projectile mass.

4. Flux estimates

Here we estimate first the average flux of interplanetary dust at 1 AU near the Moon, using the IMEM model. This model (Dikarev et al., 2005) provides a direct estimate for the (gravitationally unfocused) cumulative number flux of interplanetary dust projectiles at 1 AU, shown in Fig. 6 vs. projectile mass. The formula of Colombo et al., 1966 (with the correction outlined by Spahn et al., 2006) was used to estimate the effect of gravitational focusing by the Earth and by the Moon. It turns out that both bodies have a minor effect on the flux. Given the proposed orbit of the DSG, any enhancements/shielding due to the Moon are smaller than the general uncertainties in the model. For low altitude orbits however, the Moon may have a shielding effect, which has not been taken into account here.

The information from Fig. 6 is shown again in Fig. 7, where projectile mass has been converted to radius, assuming a density of 3000 kg m^{-3}. This number flux translates into a mass flux of roughly 2×10^{-16} kg m^{-2} s^{-1}, which is dominated by projectiles with masses larger than about 10^{-10} kg (radii larger than roughly 25 μm).

The IMEM flux is dominated by cometary projectiles (see e.g. Fig. 2 of Krüger et al., 2019), the contribution by asteroidal dust being about two orders of magnitude lower than the cometary one. In total, the IMEM model predicts about 1000 particles larger than 0.4 μm per m^2 per year at 1AU.

There are issues with converting from mass to particle size. The density used here is a mean density, and assumes compact objects. There is a variety of evidence that particles can be either porous, or complex assemblages of many, distinct, smaller components (see earlier), or a combination of these. Whilst a mean density of 3000 kg m^{-3} may be appropriate for compact silicate grains, for cometary grains for example, there is evidence from a variety of sources that this may not be appropriate. From the Stardust mission to comet Wild-2, analysis of tracks in aerogel found that about 2/3rds of particles were well condensed, strong grains, with the other 1/3rd being more weakly bound assemblages (Hörz et al., 2006; Burchell et al, 2008b). These proportions change as particle size increased, with weakly bound particles dominating at 1 mm. Also from Stardust, Kearsley et al., 2008, reported that the density of the cometary dust detected by impact craters in foils was variable, with some well compact grains having densities of 3000–4000 kg m^{-3}, whilst others had densities lower than 1000 kg m^{-3}. This effect was size dependent, with the larger particles more likely to be weakly bound assemblages. Data from the Rosetta mission to comet Churyumov-Gerasimenko gave the density of emitted dust as (1900 ± 1100) kg m^{-3} (Rotundi et al., 2015).

The IMEM model was designed to estimate spacecraft hazard by large interplanetary particles. It was calibrated with infrared observations of the zodiacal cloud by the Cosmic Background Explorer (COBE) Diffuse Infrared Background Experiment (DIRBE) instrument, in-situ flux measurements by the dust detectors on board the Galileo and Ulysses spacecraft, and the crater size distributions on lunar rock samples retrieved by the Apollo missions. Particular uncertainties exist in the submicron range. Moreover, in its numerical simulations of the dust dynamics the model does not take into account solar radiation

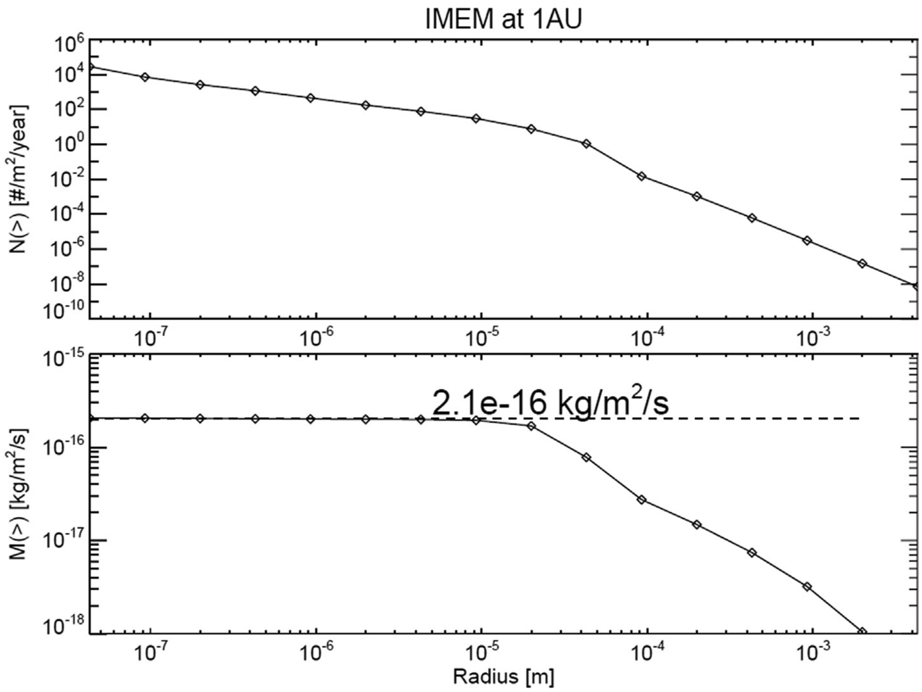

Fig. 7. Same as Fig. 6 but projectile mass is converted to radius using a density of 3000 kg m^{-3}.

pressure and the interplanetary magnetic field. These effects may lower the lifetimes of small grains and they may lead to a broadening of the directional distribution of the population of small particles. As a result, IMEM may overestimate the flux of small, submicron particles.

As a test, we compare the predicted flux to the results of Iglseder et al., 1996, who reported the lunar dust flux measured by the MDC experiment on board the Japanese HITEN spacecraft. They found, in the vicinity of the Moon, a flux of approximately 0.4 – 1.3 $\times$ 10^4 particles per m^2 per year in the size regime 10^{-19} to 10^{-10} kg. Here in Fig. 6a, we show that the current model predicts between 10^2 and 10^5 particles per m^2 per year in the same mass range, compatible with what is reported.

When considering the flux detected by any particular instrument, the instrument sensitivity has to be taken into account as well as its collection area. For example, the Cassini CDA TOF mass spectrometer had an active area of 0.008 m^2 (Srama et al., 2004), compared to 0.035 m^2 for the DDA (Krüger et al., 2019). From the IMEM model, the expected number of impacts recorded by these instruments is shown in Table 3 for various size thresholds. For relative velocities on the order of 30 km s^{-1}, during the proximal orbits of the Cassini spacecraft, CDA was sensitive to grains as small as a few tens of nanometers (Hsu et al., 2018). Here we take 0.1 μm as a conservative size threshold for potential measurements of a CDA type instrument on the Gateway. The higher mass resolution of DDA (compared to CDA) will give an even better sensitivity and we use a size threshold of 40 nm. We thus expect (from the IMEM predictions) that a CDA type instrument will record about 50 mass spectra of interplanetary particles per year, whereas a DDA type instrument will observe about 900. Similarly, the total number of impacts detectable on any passive instrument will also depend on the resolution of the analysis method used upon its return. Further, these estimates are averaged over all viewing angles. If a detector as deployed in space only views certain directions, the flux will vary depending on any directionality in the sources.

There are also other contributions to the dust flux near the Moon. Models for the dust flux near the Moon exist, e.g. Pokorny et al., 2019. As well as the direct flux of impactors, the lunar environment has a flux of dust in low altitude orbits (up to a few hundred km) that arises from ejecta thrown up from impacts on the lunar surface (Horányi et al., 2015). The contribution from this source will depend on the altitude of the orbit of the detector and will have a strong directional dependence. Horányi et al., 2015 reported the observation of a lunar dust cloud by LDEX (Lunar Dust Experiment) on the Lunar Atmosphere and Dust Environment Explorer (LADEE) orbiter mission (see also Szalay and Horányi, 2016). At 50 km altitude the dust number density for grains > 0.3 μm varied between 0.5 and 5 $\times$ 10^{-3} grains per m^3, depending on local time on the Moon. At 250 km altitude the number density varied between roughly 0.3 to 2 $\times$ 10^{-3} grains per m^3. These grains, creating a quasi-steady lunar cloud, are believed to be ejecta resulting from impacts of interplanetary projectiles on the Moon.

The dominant directions of the projectile flux seen by LDEX were reconstructed from angular variation of the ejecta that formed the cloud (Szalay and Horányi, 2016). Monthly and annual periodicity were also seen in the data.

In this way the LDEX data mapped the interplanetary flux at 1AU. The dominant populations of those interplanetary projectiles are those from the apex direction, likely originating from Halley type or Oort Cloud comets with expected impact velocities of about 60 km s^{-1}, as well as a helion (apparently coming from the Sun) and anti-helion (approaching from the anti-Sun direction) contribution, likely due to Encke-type comets or even due to 2P/Encke itself. The interplanetary dust flux suggested by LDEX equates to some 7×10^{-16} kg m^{-2} s^{-1}, which is in reasonable agreement with the number of 2×10^{-16} kg m^{-2} s^{-1} from IMEM (see above).

In addition to lunar and interplanetary dust, there will be interstellar particles at 1 AU (Sterken et al., 2019). Again, this contribution will be direction dependent. It will also be time dependent, not just over the course of a year or lunar orbit etc., but also over the period of the solar magnetic cycle, due to variations in the penetration of the flux into the inner solar system (e.g. see Strub et al., 2019). Whilst these particles are typically small, they can still be detected in the passive as well as the active detectors (see Westphal et al., 2014, who report on detection of likely interstellar grains captured at less than 1.5 AU in the aerogel and aluminium foils of the Stardust Interstellar collector).

Whilst debris from human activities is not expected to be significant initially in the *cis*-lunar region, it may grow with time. For example, unless mitigation measures are undertaken, use of any solid propellants by vehicles in the region may contribute Al_2O_3 spheres into the environment (they are used to ensure an even burn of the propellant). The DSG itself, and any visiting vehicles, will shed material (which will be potential low speed debris). In addition, any impacts of cosmic dust on the DSG can generate secondary ejecta which can in turn impact a dust detector. This can cause an elevated apparent flux, and will have to be identified in subsequent analysis. For example, Hörz et al., 2000, report clusters of tracks in aerogel from the orbital debris collector (ODC) experiment on Mir in the 1990s. These tracks all had a similar pointing direction in the aerogel, and they associated them with secondary ejecta from a primary impact on Mir. By contrast, Kearsley et al., 2005a, did not find similar clusters when analyzing HST solar cells for impact features, and thus discounted impacts on the main HST body as a significant source of secondary impacts.

It is also possible to estimate the flux of larger particles at 1 AU (in this context larger means 10 cm plus sizes). This could be done on DSG by observing impact generated light flashes on the lunar surface. Such lunar impact flashes have been observed from Earth (e.g. Dunham et al., 2000; Ortiz et al., 2006). Interpreting the impact energy (and hence impactor mass) requires knowledge of the luminous efficiency η (the fraction of incident kinetic energy that is converted into light during the impact – see Table 3 in Burchell et al., 2010 for a summary of estimates of η). This can be estimated (and compared to fluxes from lunar seismic data and counting of freshly observed craters, e.g. Oberst et al., 2012) to produce a flux for larger impactors. Whilst this has traditionally been done using ground based telescopes on Earth, it could be done from lunar orbit (e.g. see Siraj and Loeb, 2020).

5. Model payloads

Based on general principles, it is possible to define the requirements of a model payload and the potential science yield. An ideal detector should be able to respond to, and separate out, the impact sources identified in Table 1, and the particle properties shown in Fig. 1. It should also cover a wide range of particle sizes (masses) and impact speeds (see Table 2). As can be seen in Table 2, no single technology covers the whole range of requirements. Therefore it is likely to require a combination of methods with proven heritage (and hence reduced cost, more rapid deployment). As has been noted before, when the platform is to be retrievable, it would be advantageous to combine active and passive detectors (e.g. Grün et al., 2012). We recommend the inclusion of a TOF impact ionisation detector as the active component, and aerogel and metal surfaces or foils to act as the passive component. The active component would provide real-time data during a mission on particles up to a micron in size. The passive components would need retrieval, but offer a richer analysis opportunity and cover the size range from micron to mm. For the TOF spectrometer, simultaneous trajectory information combined with the compositional information would allow a link of the particle's composition to its source. Further, both an anion and cation mode of operation is of special scientific interest for the TOF spectrometer. This is because not all materials preferentially form positive ions, for example some materials favour anions (e.g. S, O and Cl, see Stephan 2001) and in addition many characteristic function groups of organic molecules also favour anions (e.g. carbon–nitrogen bonds). A high resolution TOF spectrometer would also provide complementary information to the Europa and Destiny + space missions which will carry impact TOF spectrometers. If several such instruments were active simultaneously in different parts of the Solar System, the various contributions to the dust complex (e.g. cometary, asteroidal, interstellar) can be better disentangled. As also indicated in the discussions of passive detectors and flux, the available detection area and exposure time will also be critical mission parameters, along with the pointing history of the detector components. A quartz microbalance should also be considered an essential component, to distinguish orbital debris from naturally occurring micrometeoroids and thus to help monitor the local environment. As stated, the local environment will become polluted with time, so monitoring it will be vital.

On the DSG, externally mounted payloads will likely be on pallets. These will typically be rectangular, with sizes on the order of 60 cm × 40 cm × 40 cm. A simple division is to place a TOF impact ionisation detector at one end, and the passive detectors (foils, metal surfaces and aerogel) at the other (Fig. 8). Ideally, the impact ionisation detector would be provided with a tilting mechanism and be mounted on a rotating base. It would thus act like a telescope, with its viewing direction adjusted on command. It would have a diameter and depth of some 20–30 cm. Partly to stop the passive detector being shadowed (i.e. restricted viewing angle in Fig. 8a) by the ionisation detector, it may be necessary to mount the passive component above the level of the base plane (Fig. 8b) – in which case the electronic box (not shown in Fig. 8) needed for the active ionisation detector could be placed beneath the passive component to make the best use of space. Fig. 8c shows a top view of both of these arrangements. The sides of the electronics box could be used as radiators for thermal control. Equally, the passive component could be mounted on the sides of the electronic box, giving a different viewing angle. It is possible to have more than one passive component, and these can be arranged for example to have different viewing directions (e.g. Fig. 9). If the impact ionisation detector was made slightly smaller, two such devices could be installed, one permanently biased to record positive ion time of flight mass spectra, and the other in negative ion mode. If only one such detector were deployed, it should preferably be switchable between operating modes. The pallet should also contain a quartz microbalance.

The pallet itself and exposed surfaces of any structures (including any lid for the pallet) will also be exposed to impacts. These surfaces should therefore not only be cleaned pre-flight but, unless thermal control is required, also be finished with a smooth polished surface, smooth in this context being at the micron scale to permit the identification and study of impact features down to a few microns in size. This will provide extra coverage for impact cratering experiments, increasing the total area exposed. The exterior of the ionisation detector will also provide extra passive detection area for impacts.

As stated above, for the active component, an impact ionisation detector with a TOF mass spectrometry capability is ideal, providing not just flux, but also composition for particles sizes up to around a few microns. As shown in Table 3, the detected annual flux is the combination of the impact flux and the sensitive area, and near the Moon reasonable sized instruments which could fit onto a typical pallet, will provide usable levels of impacts.

Table 3
Number of dust mass spectra expected for CDA and DDA impact ionisation instruments of various geometric detector area A_{SENS} at 1AU, estimated from the IMEM model. Highlighted in bold italics are the numbers we adopt for the plausible size thresholds of these instruments.

	CDA	DDA
A_{SENS} [m^2]	0.0080	0.0310
N(>2.0 μm) [1/A_{SENS}/year]	1	5
N(>0.4 μm) [1/A_{SENS}/year]	9	35
N(>0.1 μm) [1/A_{SENS}/year]	***56***	220
N(>0.04 μm) [1/A_{SENS}/year]	224	***868***

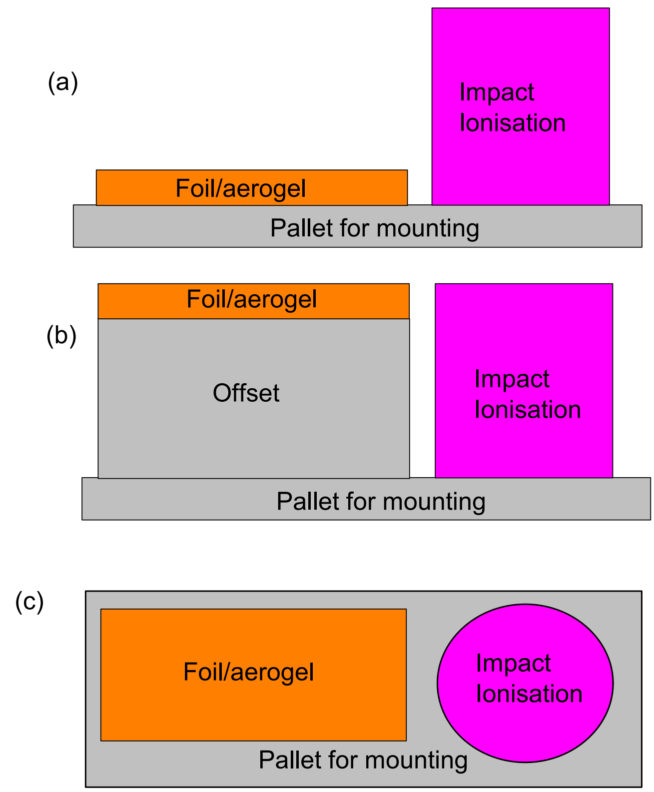

Fig. 8. Possible side view of pallet for DSG with model payload with passive (foil, aerogel) and active components (impact ionisation) detectors. (a) Shows the passive detector mounted directly onto the pallet base and with an upward view of space for its active area. (b) Shows the passive component raised up to avoid shadowing by the active detector. The impact ionization detector shown is a cylinder where the particles enter the circular top. (c) Top view compatible with both (a) and (b). Note that the impact ionisation detector will typically have a rotating base and a Y shaped yolk or a tilting mechanism to enable pointing to be determined on command.

For the passive detector, we can make a similar estimate of the number of detectable impacts. If we assume half the pallet surface is available for a suite of passive detectors, and of that about half of that is deliberately prepared and exposed surfaces (as distinct from passive structural surfaces which may have been polished to record impacts), then the specialist passive detectors could have 600 cm^2 exposed surface. With a flux of some 10^3 m^{-2} yr^{-1} for interplanetary dust particles greater than of order 1 μm in radius (Fig. 7a), the specialist passive detectors would receive around 59 impacts a year, with around 3 – 5 impacts per year of particles with radii greater than 10 μm. With an ideal design, it may be possible to achieve of order 1000 cm^2 exposed area (and hence slightly greater observed numbers of impacts), but it should be noted that this would be split across polished surfaces, foils and aerogel, so no one technology would experience the whole flux.

In addition to the dedicated dust detection instruments on the dust science pallet itself, other parts of the DSG could be utilised to provide dust flux measurements. For example, the DSG will have solar panels and if the exterior

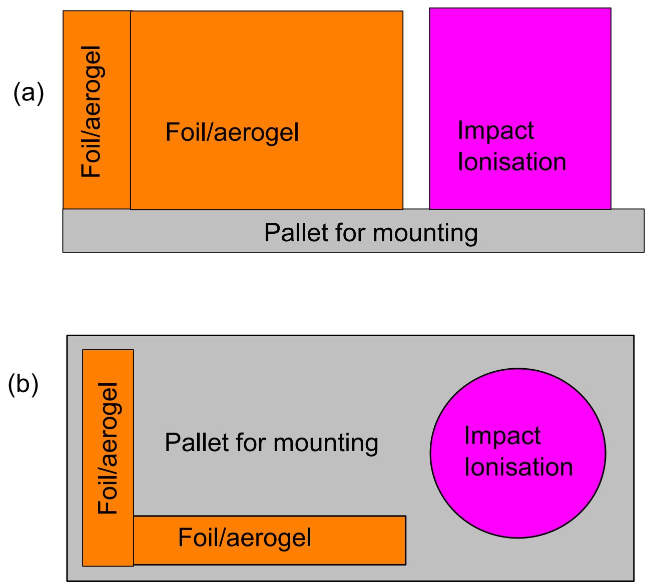

Fig. 9. An alternate configuration for a model payload. The side view is shown in (a) and the top view in (b). As well as an impact ionisation detector (right), there are two passive detectors (left), each mounted edge on to the payload pallet but orthogonal to each other. The active surface of each passive detector faces outwards and sideways, sampling different impact directions.

of the DSG were equipped with a robotic arm and high resolution camera, the surfaces of these panels could conceivably be surveyed at regular intervals. As already stated, the impact damage to glass is distinctive (Fig. 3), the central pit is surrounded by a much larger conchoidal fracture zone (of order 100× impactor size). Given the exposure of the solar panels would be anticipated to be much longer than individual science payloads, then if cm-sized features were detectable by such a camera system, this would measure the flux of >100 µm particles. From Fig. 7a, the IMEM flux model predicts the annual flux of 100 µm particles to be of order 10^{-2}, implying one such impact a year per 100 m^2 of solar panels.

Similarly, if there was a radio science pallet, serendipitous use could be made of any RF antenna to detect the plasma pulse arising from the local impact of a dust grain (see 3.11 above).

Finally, as already noted, if the DSG were equipped with a telescope to study the lunar surface, this could also be tasked to detect the light flash arising from an impact on the lunar surface. If such impacts were noted and the coordinates revisited for high resolution optical surveys, this would also permit an inventory to be built up of fresh lunar impact craters by high resolution cameras on-board missions such as the Lunar Reconnaissance Orbiter (c.f. fresh crater identified on Mars by the Mars Global Surveyor e.g. Malin et al., 2006 and subsequently by Mars Reconnaissance Orbiter e.g. McEwen et al., 2007; Daubar et al., 2013). This would also increase the size range of objects measured from the small (dust) regime to larger cm scales and beyond. If modelling of the craters permits estimates of the impactor size, it would also constrain the luminous efficiency coefficient η (see Section 4).

Overall therefore, there are strong reasons to deploy a suite of dust detectors in the vicinity of the Moon. The technologies required are mature. A retrievable pallet offers the best science return permitting detailed size (flux) and compositional studies of dust grains over a range of sizes from 10 s of nm (via impact ionisation time of flight mass spectroscopy) up to a few mms (from captured grains in aerogel, or residues and fragments on foils and metal surfaces).

6. Conclusions

The proposal to build a new space station near the Moon, offers many opportunities for science. One of these is to observe the dust flux to benefit both scientific enquiry and better understand the hazard interplanetary dust represents for space vehicles (e.g. Grün et al., 2019). A platform which incorporates an impact ionisation detector will permit the study of mass spectra of micron and sub-micron dust at 1 AU. Differentiating between the compositions of the different components of the dust flux has been a major source of scientific discoveries wherever such detectors have been deployed in space. In addition, if combined with a set of passive detectors designed to be retrieved after exposure for study here on Earth, this will mean the size range of dust from a few tens of nm to mm scale will be accessible. If no retrieval were possible, other types of active detector are described which can provide at least flux data for particles at greater than the micron scale, and if combined appropriately can provide particle speed and trajectory information as well as a basic density estimate. The various detector technologies are also sensitive to different speed ranges. Aerogel for example is more suited to impact speeds below 10 km s^{-1}, to increase the amount of material captured relatively intact. Impact ionisation is more suited to higher speeds if purely elemental lines are desired in impact mass spectra, but still operates at lower speeds, albeit requiring more statistical based analyses. Impact craters also exhibit impact speed related effects, with more residue retained at lower speeds. Combining these various technologies together in one package, thus increases the science reach of the whole instrument. Given that different dust sources will have different impact speeds at the DSG, this again suggests a range of instrument technologies is required to separate the composition of each source.

This will be the best chance to obtain a flux measurement at 1 AU near the Moon before that environment starts to become more heavily populated with the debris from space vehicles and their increased use in that locality. Indeed, the DSG itself will generate debris as time goes on, emphasising the need to deploy a dust detector suite of instruments as early as possible in the lifetime of the DSG. The combination of several technologies, including returning samples for laboratory analysis, gives maximum sensitivity over not just a wide size range but also particle compositions. Given that all these instruments already have space heritage, there need be no lengthy delay for design and testing – all are proven technologies. It is thus both feasible and highly desirable, that the DSG carries such a suite of instruments and measures the dust flux near the Moon.

Funding

We wish to thank ESA for supporting this work with a grant to organise a topical working team on this topic. MJB, PJW, MvG, JCB and LJH acknowledge support from STFC. VJS received funding from the European Union's Horizon 2020 research and innovation programme under grant agreement N°851544

5. Availability of data and material

There is no data associated with this study other than contained in the paper

6. Authors' contributions

All authors attended at least one workshop on the topic of this paper and read the manuscript, except VS who was invited to help with the science in the manuscript after the meetings. We thank the referees for their insightful comments and suggestions which improved the manuscript.

Declaration of Competing Interest

The author declare that there is no conflict of interest.

References

Alexander W.M., McCracken C.W, Secretan L., Oberg O.E. Review Of Direct Measurements Of Interplanetary Dust From Satellites And Probes. NASA N64-17609, TM-X-54570, X-613-62-25 (1962).

Auer S., Accuracy of a Velocity/trajectory Sensor for Charged Dust Particles. Astronomical Society of the Pacific Conference Series; Proceedings of the 150th colloquium of the International Astronomical Union (Gainesville; Florida; USA) 1995. Eds. B.A.S. Gustafson and M.S. Hanner: pub. Astronomical Society of the Pacific (ASP 104), 251 – 254 (1996).

Auer S. Instrumentation. Chapter 10, pp 385 – 444, in Interplanetary Dust, eds. Grün E. Gustafson B.Å.S., Dermott S.F., and Fechtig H. Pub Springer (2001). ISBN 3-540-42067-3.

Ayers, M.R., Hunt, A.J., 1998. Titanium oxide aerogels prepared from titanium metal and hydrogen peroxide. Mater. Lett. 34, 290–293.

Baguhl, M. et al., 1995. Dust Measurement at High Ecliptic Latitudes. Science 268 (5213), 1016–1019.

Barrett, R.A., Zolensky, M.E., Hörz, F., Lindstrom, D.J., Gibson, E.K., 1992. Suitability of silica aerogel as a capture medium for interplanetary dust. Proc. Lunar and Planetary Science 22, 203–212.

Bernhard, R.P., Zolensky, M.E., 1993. Analysis of impactor residues in tray clamps from the Long Duration Exposure Facility. Part 1: Clamps from Bay A of the satellite. NASA technical report TM-104759, S-708, NAS 1.15:104759 (1993).

Bridges, J.C., Burchell, M.J., Changela, H.C., Foster, N.J., Creighton, J. A., Carpenter, J.D., Gurman, S.J., Franchi, I.A., Busemann, H., 2010. Iron oxides in comet 81P/Wild 2 samples. Meteorit Planet Sci 45, 55–72.

Bridges, J.C., Changela, H.G., Nayakshin, S., Starkey, N.A., Franchi, I. A., 2012. Chondrule fragments from Comet Wild2: evidence for high temperature processing in the outer solar system. Earth Planet Sci Lett 341–344, 186–194.

Briois, C., Thissen, R., Thirkell, L., Aradj, K., Bouabdellah, A., Boukrara, A., Carrasco, N., Chalumeau, G., Chapelon, O., Colin, F., Coll, F., Cottin, H., Engrand, C., Grand, N., Lebreton, J.-P., Orthous-Daunay, F.R., Pennanech, C., Szopa, C., Vuitton, V., Zapf, P., Makarov, A., 2016. Orbitrap mass analyser for in situ characterisation of planetary environments: performance evaluation of a laboratory prototype. Planet Space Sci 131, 33–45.

Brownlee, D.E., 1985. Cosmic dust: collection and research. Ann. Rev. Earth and Planetary Sci. 13, 147–173.

Brownlee, D.E., 2014. The stardust mission: analysing samples from the edge of the solar system. Ann. Rev. Earth and Planetary Sci. 42, 179–205.

Brownlee, D. et al., 1994. Eureka!! Aerogel capture of meteoroids in space. In: 25th Lunar and Planetary Science Conference, pp. p183–p184.

Brownlee, D.E. et al., 2006. Comet wild-2 under a microscope. Science 314, 1711–1716.

Bunch, T.E., Schultz, P., Cassen, P., Brownlee, D., Podolak, M., Lissauer, J., Reynolds, R., Chang, S., 1991. Are some chondrule rims formed by impact processes? Observations and experiments. Icarus 91, 76–92.

Burchell, M.J., Mackay, N., 1998. Crater ellipticity in hypervelocity impact on metals. J. Geophys. Res. 103 E, 22761–22774.

Burchell, M.J., Thomson, R., Yano, H., 1999a. Capture of hypervelocity particles in aerogel: in ground laboratory and low earth orbit. Planet Space Sci. 47, 189–204.

Burchell, M.J., Cole, M.J., McDonnell, J.A.M., Zarnecki, J.Z., 1999b. Hypervelocity impact studies using the 2 MV Van de Graaff accelerator and two-stage light gas gun of the University of Kent at Canterbury. Meas. Sci. Technol. 10, 41–50.

Burchell, M.J., Creighton, J.A., Cole, M.J., Mann, J., Kearsley, A.T., 2001. Capture of particles in hypervelocity impacts in aerogel. Meteorit Planet Sci. 36, 209–221.

Burchell, M.J., Creighton, J.A., Kearsley, A.T., 2004. Identification of organic particles via Raman techniques after capture in hypervelocity impacts on aerogel. J. Raman Spectrosc 35, 249–253.

Burchell, M.J., Graham, G., Kearsley, A.T., 2006a. Cosmic dust collection in aerogel. Annual Reviews of Earth and Planetary Science 34, 385–418.

Burchell, M.J., Mann, J., Creighton, J.A., Kearsley, A.T., Graham, G., Franchi, I.A., 2006b. Identification of minerals and meteoritic materials via raman techniques after capture in hypervelocity impacts on aerogel. Meteorit Planet Sci. 41, 217–232.

Burchell, M.J., Foster, N.J., Kearsley, A.T., Creighton, J.A., 2008a. Identification of mineral impactors in hypervelocity impact craters in aluminium by raman spectroscopy of residues. Meteorit Planet Sci. 43, 135–142.

Burchell, M.J., Fairey, S.A.J., Wozniakiewicz, P., Brownlee, D.E., Hörz, F., Kearsley, A.T., See, T.H., Tsou, P., Westphal, A., Green, S.F., Trigo-Rodríguez, J.M., Dominguez, G., 2008b. Characteristics of cometary dust tracks in stardust aerogel and laboratory calibrations. Meteorit Planet Sci. 43, 23–40.

Burchell, M.J., Creighton, J.A., Cole, M.J., Mann, J., Kearsley, A.T., 2009a. Hypervelocity capture of particles in aerogel: dependence on aerogel properties. Planet Space Sci. 57, 58–70.

Burchell, M.J., Foster, N.J., Ormond-Prout, J., Dupin, D., Armes, S.P., 2009b. Extent of thermal ablation suffered by model organic microparticles during aerogel capture at hypervelocities. Meteorit Planet Sci. 44 (10), 1407–1419.

Burchell, M.J., Robin-Williams, R., Foing, B.H., 2010. and the SMART-1 Impact Team. The SMART-1 Lunar Impact. Icarus 207, 28–38.

Burchell, M.J., Standen, S., Cole, M.J., Corsaro, R.D., Giovane, F., Liou, J.-C., Pisacane, V., Sadelik, A., Stansbery, E., 2011. Acoustic response

of aluminium and Duroid plates to hypervelocity impacts. Int. J. Impact Eng. 38, 426–433.
Burchell, M.J., Armes, S.P., 2011. Impact ionization spectra from aliphatic PMMA microparticles. Rapid Communications in Mass Spectroscopy 25, 543–550.
Burchell, M.J., Cole, M.J., Price, M.C., Kearsley, A.T., 2012. Experimental investigation of impacts by solar cell secondary ejecta on silica aerogel and aluminium foil: implications for the Stardust Interstellar Dust Collector. Meteorit Planet Sci. 47, 671–683.
Burchell, M.J., Corsaro, R., Giovane, F., Cole, M.J., Sadelik, A., Price, M.C., Liou, J.-C., 2013. A New Cosmic Dust Detector with a Novel Method using a Resistive Grid Sensitive to Hypervelocity Impacts. Procedia Eng. 58, 68–76.
Cohen, B.A., Szalay, J.R., Rivkin, A.S., Richardson, J.A., Klima, R.L., Ernst, C.M., Chabot, N.L., Sternovsky, Z., Horanyi, M., 2019. Using dust shed from asteroids as microsamples to link remote measurements with meteorite classes. Meteorit Planet Sci. 54 (9), 2046–2066.
Colombo, G., Lautman, D.A., Shapiro, I.I., 1966. The Earth's Dust Belt: Fact or fiction?: 2. Gravitational focusing and Jacobi capture. J. Geophys. Res. 71 (2), 5705–5717. https://doi.org/10.1029/JZ071i023p05705.
Crusan J., Bleacher J., Caram J., Craig D., Goodliff K., Hermann N., Mahoney E., Smith M. NASA's Gateway: An Update on Progress and Plans for Extending Human Presence to Cislunar space. 2019 IEEE Aerospace Conference. IEEE Aerospace Conference Proceedings, 19pp. (2019). ISSN 1095-323X.
Dahlmann, B.K., Grün, E., Kissel, J., Dietzel, H., 1977. The ion composition of the plasma produced by impacts of fast dust particles. Planet Space Sci. 25, 135–147.
Daubar, I.J., McEwen, A.S., Byrne, S., Kennedy, M.R., Ivanov, B., 2013. The current martian cratering rate. Icarus 225, 506–516.
Della Corte V., et al. GIADA: shining a light on the monitoring of the comet dust production from the nucleus of 67P/Churyumov-Gerasimenko. A. & A. 583, A13 (10 pp) (2015).
Della, C.V. et al., 2019. GIADA microbalance measurements on board Rosetta: submicrometer- to micrometer-sized dust particle flux in the coma of comet 67P/Churyumov-Gerasimenko. A. & A. 630, A25.
Dietzel, H., Eichhorn, G., Fechtig, H., Grün, E., Hoffman, H.-J., Kissel, J., 1973. The HEOS2 and Helios micrometeoroid experiments. J. Phys. E: Sci. Instrum. 6, 209–217.
Dikarev, V., Grün, E., Baggaley, J., Galligan, D., Landgraf, M., Jehn, R., 2005. The new ESA meteoroid model. Adv. Space Res. 35, 1282–1289. https://doi.org/10.1016/j.asr.2005.05.014.
Dirri, F., Palomba, E., Longobardo, A., Zampetti, E., Saggin, B., Scaccabarozzi, D., 2019. A review of quartz crystal microbalances for space applications. Sens. Actuators, A: Phys. 287, 48–75.
Doyle, H.M., Tom, J.G., Nogacek, K.H., Anderson, C.R., Kang, J.S., 2016. Design and Development of DRAGONS In-situ Orbital Debris Detection and Characterization Payload. Trans. Japan Soc. Aero. Space Sci. 59 (4), 218–225.
Drolshagen, G., McDonnell, J.A.M., Stevenson, T.J., Despande, S., Kay, L., Tanner, W.G., Mandeville, J.C., Carey, W.C., Maag, C.R., Griffiths, A.D., Shrine, N.G., Aceti, R., 1995. Optical survey of micrometeoroid and space debris impact features on EURECA. Planet Space Sci 44 (4), 317–340.
Drolshagen, G., Carey, W.G., McDonnell, J.A.M., Stevenson, T.J., Mandeville, J.C., Berthoud, L., 1997. HST Solar Array Impact Survey: Revised Damage Laws and Residue Analysis. Adv. Space Rev. 19 (2), 239–251.
Dunham, D.W., Cudnik, B., Palmer, D.M., Sada, P.V., Melosh, J., Frankenberger, M., Beech, R., Pelerin, L., Venable, R., Asher, D., Sterner, R., Gotwols, B., Wun, B., Stockbauer, D., 2000. The First Confirmed Video Recordings of Lunar Meteor Impacts. Lunar and Planetary Science Conference XXXI, abstract 1547.
Faure, P., Masuyama, S., Nakamoto, H., Akahoshi, Y., Kitazawa, Y., Koura, T., 2013. Space Dust Impacts Detector Development for the Evaluation of Ejecta. Procedia Eng 58, 594–600.
Fechtig H., Leinert C, and Berg O.E. Historical Perspectives. Chapter 1, pp 1 – 56, in Interplanetary Dust, eds. Grün E. Gustafson B.Å.S., Dermott S.F., and Fechtig H. Pub Springer (2001). ISBN 3-540-42067-3.
Fiege, K., Trieloff, M., Hillier, J.K., Guglielmino, M., Postberg, F., Srama, R., Kempf, S., Blum, J., 2014. Calibration of relative sensitivity factors for impact ionization detectors with high-velocity silicate microparticles. Icarus 241, 336–345.
Flynn G.J., Horz F., Bajt S., Sutton S.R. In-Situ Chemical Analysis of Extraterrestrial Material Captured in Aerogel, Lunar and Planetary Science. 27th Annual Lunar and Planetary Science Conference, abstracts vol. 27, 369 - 370 (1996).
Flynn, G. et al., 2014. Stardust Preliminary Examination VII: Synchrotron X-ray Fluorescence Analysis of Six Stardust Interstellar Candidates measured with the Advanced Photon Source 2-ID-D Microprobe. Meteorit Planet Sci 49, 1626–1644.
Gardner, D.J., Collier, I., Shrine, N.R.G., Griffiths, A.D., McDonnell, J.A.M., 1996. Micro-Particle Impact Flux on the Timeband Capture Cell Experiment Of The EuReCa Spacecraft. Adv. Space Res. 17 (12), 193–199.
Gardner, D.J., McDonnell, J.A.M., Collier, I., 1997. Hole Growth Characterisation for Hypervelocity Impacts in Thin Targets. Int. J. Impact Engng. 19 (7), 589–602.
Goldsworthy, B.J., Burchell, M.J., Cole, M.J., Green, S.F., Leese, M.R., McBride, N., McDonnell, J.A.M., Müller, M., Grün, E., Srama, R., Armes, S.P., Khan, M.A., 2002. Laboratory Calibration of the Cassini Cosmic Dust Analyser (CDA) Using New, Low Density Projectiles. Adv Space Res 29, 1139–1144.
Goldsworthy, B.J., Burchell, M.J., Cole, M.J., Armes, S.P., Khan, M.A., Lascelles, S.F., Green, S.F., McDonnell, J.A.M., Srama, R., Bigger, S.W., 2003. Time of Flight Mass Spectrometry of Ions in Plasmas Produced by Hypervelocity Impacts of Organic and Mineralogical Microparticles on a Cosmic Dust Analyser. A & A 409, 1151–1167.
Göller, J.R., Grün, E., 1989. Calibration of the Galileo Ulysses Dust Detectors with Different Projectile Materials and at Varying Impact Angles. Planet Space Sci 37, 1197–1206.
Graham, G.A., Kearsley, A.T., Wright, I.P., Burchell, M.J., Taylor, E.A., 2003. Observations on hypervelocity impact damage sustained by multi-layered insulation foils exposed in low Earth orbit and simulated in the laboratory. Int J Impact Eng 29, 307–316.
Grün, E. et al., 1993. Discovery of Jovian Dust Streams and Interstellar Grains by the Ulysses Spacecraft. Nature 362 (6419), 428–430.
Grün E., Gustafson B.A.S., Dermott S., and Fechtig H. (Eds.). Interplanetary Dust. Pub. Springer, pp.804 (2001). DOI: 10.1007/978-3-642-56428-4.
Grün, E. et al., 2012. Active Cosmic Dust Detector. Planet Space Sci 60 (1), 261–273.
Grün E, Krüger H., Srama R. The Dawn of Dust Astronomy. Space Sci. Rev. 215:46 (51 pp) (2019).
Gurnett, D.A., Grün, E., Gallagher, D., Kurth, W.S., Scarf, F.L., 1983. Micron-sized particles detected near Saturn by the Voyager plasma wave instrument. Icarus 53, 236–254.
Hicks, L.J., MacArthur, J., Bridges, J.C., Price, M., Wickham-Eade, J., Burchell, M., Hansford, G., Butterworth, A., Gurman, S.J., Baker, S., 2017. Magnetite in Comet Wild 2: Evidence for parent body aqueous alteration. Meteorit. Planet. Sci. 52 (10), 2075–2096. https://doi.org/10.1111/maps.12909.
Hillier, J.K., Sestak, S., Green, S.F., Postberg, F., Srama, R., Trieloff, M., 2009. The production of platinum-coated silicate nanoparticle aggregates for use in hypervelocity impact experiments. Planet Space Sci 57 (14–15), 2081–2086.
Hillier, J.K., Postberg, F., Sestak, S., Srama, R., Kempf, S., Trieloff, M., Sternovsky, Z., Green, S.F., 2012. Impact ionization mass spectra of anorthite cosmic dust analogue particles. J Geophys Res 117, E09002. https://doi.org/10.1029/2012JE004077.
Hillier, J.K., Sternovsky, Z., Armes, S.P., Fielding, L.A., Postberg, F., Bugiel, S., Drake, K., Srama, R., Kearsley, A.T., Trieloff, M., 2014.

Impact ionisation mass spectrometry of polypyrrole-coated pyrrhotite microparticles. Planet Space Sci 97, 9–22.
Hillier, J.K., Sternovsky, Z., Kempf, S., Trieloff, M., Guglielmino, M., Postberg, F., Price, M.C., 2018. Impact ionisation mass spectrometry of platinum-coated olivine and magnesite-dominated cosmic dust analogues. Planet Space Sci 156, 96–110.
Hirai, T., Cole, M.J., Fujii, M., Hasegawa, S., Iwai, T., Kobayashi, M., Srama, R., Yano, H., 2014. Microparticle impact calibration of the Arrayed Large-Area Dust Detectors in Interplanetary space (ALADDIN) onboard the solar power sail demonstrator IKAROS. Planet Space Sci 100, 87–97.
Horányi, M., Szalay, J.R., Kempf, S., Schmidt, J., Grün, E., Srama, R., Sternovsky, Z., 2015. A permanent, asymmetric dust cloud around the Moon. Nature 522, 324–326.
Hornung, K., Kissel, J., 1994. On Shock Wave Impact Ionization of Particles. A & A 291, 324–336.
Hörz F., Bernard R.P., Warren J., See T.H., Brownlee D.E., Laurance M. R., Messenger S. and Peterson R.B. Preliminary analysis of LDEF instrument A0187-1 'Chemistry of Micrometeoroids Experiment'. In LDEF – 69 months in space, first post-retrieval symposium, NASA conference publication 3134, part 1, 487-502 (1993).
Hörz, F., Zolensky, M.E., Bernhard, R.P., See, T.H., Warren, J.L., 2000. Impact features and projectile residues in aerogel exposed on Mir. Icarus 147, 559–579.
Hörz, F. et al., 2006. Impact features on the Stardust Collector and implications for Wild 2 Coma Dust. Science 314, 1716–1719.
Hsu, H.-W. et al., 2018. In situ collection of dust grains falling from Saturn's rings into its atmosphere. Science 362 (6410), eaat3185.
Humes, D.H., 1993. Large craters on the meteoroid and space debris impact experiment. In *LDEF – 69 months in space, first post-retrieval symposium*. NASA Conf Publ**3134**, part 1, 399–418.
Iglseder, H., Uesugi, K., Svedhem, H., 1996. Cosmic Dust Measurements in Lunar Orbit. Adv Space Res 17 (12), 177–182.
Ikari S., et al. Solar System Exploration Sciences by EQUULEUS on SLS EM-1 and Science Instruments Development Status. 33rd Annual AIAA/USU Conference on Small Satellites, Utah, USA (2019).
Ishii H.A., Brennan S., Bradley J.P., Pianetta P., Kearsley A.T., Burchell M.J. Sulfur Mobilization In Stardust Impact Tracks. Lunar and Planetary Science XXXIX, abstract 1561 (2008a).
Ishii, H.A., Brennan, S., Bradley, J.P., Luening, K., Ignatyev, K., Pianetta, P., 2008b. Recovering the elemental composition of comet Wild 2 dust in five Stardust impact tracks and terminal particles in aerogel. Meteorit Planet Sci 43, 215–231.
Jones, S., Flynn, G., 2011. Hypervelocity Capture of Meteoritic Particles in Non-Silica Aerogel. Meteorit Planet Sci 46 (9), 1253–1264.
Joswiak, D.J., Nakashima, D., Brownlee, D.E., Matrajt, G., Ushikubo, T., Kita, N.T., Messenger, S., Ito, M., 2014. Terminal particle from Stardust track 130: Possible Al-rich chondrule fragment from comet Wild 2. Geochim Cosmochim Acta 144, 277–298.
Kempf, S., Srama, R., Altobelli, N., Auer, S., Tschernjawski, V., Bradley, J., Burton, M.E., Helfert, S., Johnson, T.V., Krüger, H., Moragas-Klostermeyer, G., Grün, E., 2004. Cassini between Earth and asteroid belt: first in-situ charge measurements of interplanetary grains. Icarus 171, 317–335.
Kearsley, A.T., Graham, G.A., 2004. Multi-layered foil capture of micrometeoroids and orbital debris in low Earth orbit. Adv Space Res 34, 939–943.
Kearsley, A.T., Drolshagen, G., McDonnell, J.A.M., Mandeville, J.C., Moussi, A., 2005a. Impacts on Hubble Space Telescope solar arrays: Discrimination between natural and man-made particles. Adv. Spa. Res. 35, 1254–1262.
Kearsley, A.T., Graham, G.A., Burchell, M.J., Taylor, E.A., Drolshagen, G., Chater, R.J., McPhail, D., 2005b. MULPEX: A compact multi-layered polymer foil collector for micrometeoroids and orbital debris. Adv Space Res 35, 1270–1281.
Kearsley A.T., Graham G.A., Burchell .J., Cole M., Drolshagen G., Chater R.J. and McPhail D.S. Sampling the orbital debris population using a foil residue collector in a standardised container for experiments (SCE). Proceedings of the 4th European Conference on Space Debris. ESA/ESOC, Darmstadt, Germany, (ESA SP-587) (2005c).
Kearsley, A.T., Burchell, M.J., Hörz, F., Cole, M.J., Schwandt, C.S., 2006. Laboratory simulation of impacts on aluminium foils of the Stardust spacecraft: Calibration of dust particle size from comet Wild-2. Meteorit Planet Sci 41, 167–180.
Kearsley, A.T., Graham, G.A., Burchell, M.J., Cole, M.J., Dai, Z., Teslich, N., Chater, R.J., Wozniakiewicz, P.J., Spratt, J., Jones, G., 2007a. Analytical scanning and transmission electron microscopy of laboratory impacts on Stardust aluminium foils: interpreting impact crater morphology and the composition of impact residues. Meteorit Planet Sci 42, 191–210.
Kearsley, A.T., Graham, G.A., McDonnell, J.A.M., Taylor, E.A., Drolshagen, G., Chater, R.J., McPhail, D., Burchell, M.J., 2007b. The Chemical Composition of Micrometeoroids Impacting Upon the Solar Arrays of the Hubble Space Telescope. Adv Space Res 39, 590–604.
Kearsley, A.T., Borg, J., Graham, G.A., Burchell, M.J., Cole, M.J., Leroux, H., Bridges, J.C., Horz, F., Wozniakiewicz, P.J., Bland, P.A., Bradley, J.P., Dai, Z.R., Teslich, N., See, T., Hoppe, P., Heck, P.R., Huth, J., Stadermann, F.J., Floss, C., Marhas, K., Stephan, T., Leitner, J., 2008. Dust from comet Wild 2: Interpreting particle size, shape, structure, and composition from impact features on the Stardust aluminium foils. Meteorit Planet Sci 43, 41–73.
Khawaja, N., Postberg, F., Hillier, J., Klenner, F., Kempf, S., Nölle, L., Reviol, R., Zou, Z., Srama, R., 2019. Low-mass nitrogen-, oxygen-bearing, and aromatic compounds in Enceladean ice grains. MNRAS 489, 5231–5243. https://doi.org/10.1093/mnras/stz2280.
Kissel, J., Krueger, F.R., Silén, J., Clark, B.C., 2004. The Cometary and Interstellar Dust Analyzer at Comet 81P/Wild2. Science 304 (5678), 1774–1776.
Kitazawa, Y., Fujiwara, A., Kadano, T., Imagawa, K., Okada, Y., Uematsu, K., 1999. Hypervelocity impact experiments on aerogel dust collector. J. Geophys. Res. 104 (E9), 22035–22052.
Kobayashi, M., Krüger, H., Senshu, H., Wada, K., Okudaira, O., Sasaki, S., 2018. Kimura H In situ observations of dust particles in Martian dust belts using a large-sensitive-area dust sensor. Planet Space Sci 156, 41–46.
Krüger, H. et al., 2006. Galileo Dust Data from the Jovian System 1997–1999. Planet Space Sci 54, 879–910.
Krüger, H., Strub, P., Srama, R., Kobayashi, M., Arai, T., Kimura, H., Hirai, T., Moragas-Klostermeyer, G., Altobelli, N., Sterken, V.J., Agarwal, J., Sommer, M., Grün, E., 2019. Modelling DESTINY+ interplanetary and interstellar dust measurements en route to the active asteroid (3200) Phaethon. Planet Space Sci 172, 22–42.
Lange, G., Jessberger, E.K., Aigner, S., Igenbergs, E., Kuczera, H., Maas, D., Sutton, S., Weishaupt, U., Zinner, E., 1986. Chemical fractionation effects during high velocity impact. Adv Space Res 6, 9–12.
Li, X., He, H., Ren, L., 2017. Fabrication and characterization of the monolithic hydrophobic alumina aerogels. J. Porous Mater. 24, 679–683.
Liu, B., Gao, M., Liu, X., Xie, Y., Yi, X., Zhu, L., Wang, X., Shen, X., 2018. Monolithic zirconia aerogel from polyacetylacetonatorirconium precursor and ammonia hydroxide gel initiator: formation mechanism, mechanical strength and thermal properties. Royal Society of Chemistry Advances 8, 41603–41611.
Liou, J.C., Corsaro, R., Giovane, F., Anderson, C., Sadilek, A., Burchell, M., Hamilton, J., 2015. and the DRAGONS team. DRAGONS – A Micrometeoroid and Orbital Debris Impact Sensor. In: International Symposium on Space Technology.
Love, S.G., Brownlee, D.E., King, N.L., Horz, F., 1995. Morphology of Meteoroid and Debris Impact Craters Formed in Soft Metal Targets on the LDEF Satellite. Int. J. Impact Eng.. 16 (3), 403–418.
Maag C., Linder W.K. Results of space shuttle intact particle experiments. In Hypervelocity Impacts in Space, pp. 186-190. Ed J.A.M. McDonnell, pub. Univ. of Kent, 228 pages (1992). ISBN 0904938328.

Malin, M.C., Edgett, K.S., Posiolova, L.V., McColley, S.M., Dobrea, E. Z.N., 2006. Present-day impact cratering rate and contemporary gully activity on Mars. Science 314, 1573–1577.

Mandeville, J.C., 1991. Study of cosmic dust particles on board LDEF: the Frecopa experiment. Adv. Space Res. 11 (12), 12101–12107.

Mandeville J.C. and Borg J. Study of cosmic dust particles on board LDEF: The FRECOPA experiments A0138-1 and A0138-2. In LDEF – 69 months in space, first post-retrieval symposium, NASA conference publication 3134, part 1, 419 – 434 (1993).

Mann, I., Nouzák, L., Vaverka, J., Antonsen, T., Fredriksen, A., Issautier, K., Malaspina, D., Meyer-Vernet, N., Pavlu, J., Sternovsky, Z., Stude, J., Ye, S., Zaslavsky, A., 2019. Dust observations with antenna measurements and its prospects for observations with Parker Solar Probe and Solar Orbiter. Ann. Geophys. 37, 1121–1140.

Masanori M., Srama, R., Krüger, H., Arai, T., Kimura, H. Destiny+ dust analyser. In: Lunar and Planetary Institute Science Conference Abstracts, Volume 49 of Lunar and Planetary Institute Science Conference Abstracts, abstract #2050 (2018).

McDonnell, J.A.M., Carey, W.C., Dixon, D.G., 1984. Cosmic dust collection by the capture cell technique on the Space Shuttle. Nature 309, 237–240.

McDonnell J.A.M. and Stevenson T.J. Hypervelocity Impact Microfoil Perforations In The LEO Space Environment (LDEF, MAP AO-023 Experiment). LDEF – 60 Months in Space. First Post-Retrieval Symposium (part 1), pp. 443 - 458. Ed. Levine A. NASA Conference Publication 3134 (1991).

McDonnell, J.A.M., Gardner, D.J., 1998. Meteoroid morphology and densities: decoding satellite impact data. Icarus 133, 25–35.

McEwen A.S., Eliason E.M., Bergstrom J.W., Bridges N.T>, Hansen C.J., Delamere W.A., Grant J.A., Gulick V.C., Herkenhoff K.E., Keszthelyi L., Kirk R.L., Mellon M.T., Squyres S.W., Thomas N. and Weitz C. M. Mars Reconnaissance Orbiter's High Resolution Imaging Science Experiment (HiRISE). Journal of Geophysical Research 112, E05S02, doi:10.1029/2005JE002605 (2007).

Meyer-Vernet, N., Moncuquet, M., Issautier, K., Schippers, P., 2017. Frequency Range of Dust Detection in Space with Radio and Plasma Wave Receivers: Theory and application to Interplanetary Nanodust Impacts on Cassini. J. Geophys. Res – Space Physics 122, 8–22.

Murr, L.E., Kinard, W.H., 1993. Effects of low earth orbit. Am. Sci. 81, 152–165.

Nakamura, T., Tsuchiyama, A., Akaki, T., Uesugi, K., Nakano, T., Takeuchi, A., Suzuki, Y., Noguchi, T., 2008a. Bulk Mineralogy and Three-Dimensional Structures of Individual Stardust Particles Deduced from Synchrotron X-Ray Diffraction and Microtomography Analysis. Meteorit Planet Sci 43, 247–259.

Nakamura, T., Noguchi, T., Tsuchiyama, A., Ushikubo, T., Kita, N.T., Valley, J.W., Zolensky, M.E., Kakazu, Y., Sakamoto, K., Mashio, E., Uesugi, K., Nakano, T., 2008b. Chondrule like objects in short-period Comet 81P/Wild 2. Science 321, 1664–1667.

Nakamura, M., Kitazawa, Y., Matsumoto, H., Okudaira, K., Hanada, T., Sakurai, A., Funakoshi, K., Yasaka, T., Hasegawa, S., Kobayashi, M., 2015. Development of in-situ micro-debris measurement system. Adv. Spa. Res. 56, 436–448.

Neish M.J., Kitazawa Y., Noguchi T., Inoue T., Imagawa K., Goka T., Ochi S. Passive Measurement of Dust Particles on the ISS Using MPAC: Experiment Summary, Particle Fluxes and Chemical Analysis. Proceedings of the 4th European Conference on Space Debris (ESA SP-587). 18-20 April 2005, ESA/ESOC, Darmstadt, Germany. Editor: D. Danesy, p.221 – 226 (2005).

Nogami, K., Fujii, M., Ohashi, H., Miyachi, T., Sasaki, S., Hasegawa, S., Yano, H., Shibata, H., Iwai, T., Minami, S., Takechi, S., Grün, E., Srama, R., 2010. Development of the Mercury dust monitor (MDM) onboard the BepiColombo mission. Planet Space Sci 58, 108–115.

Noguchi, T., Nakamura, T., Okudaira, K., Yano, H., Sugita, S., Burchell, M.J., 2007. Thermal alteration of hydrated minerals during hypervelocity capture to silica aerogel at the flyby speed of STARDUST. Meteorit Planet Sci 42, 357–372.

Oberst, J., Christou, A., Suggs, R., Moser, D., Daubar, I.J., McEwen, A. S., Burchell, M., Kawamura, T., Hiesinger, H., Wünnemann, K., Wagner, R., Robinson, M.S., 2012. The present-day flux of large meteoroids on the lunar surface—A synthesis of models and observational techniques. Planet Space Sci 74, 179–193.

Ortiz, J.L., Aceituno, F.J., Quesada, J.A., Aceituno, J., Fernandez, M., Santos-Sanz, P., Trigo-Rodriguez, J.M., Llorca, J., Martin-Torres, F. J., Montanes-Rodriquez, P., Palle, E., 2006. Detection of sporadic impact flashes on the Moon: implications for the luminous efficiency of hypervelocity impacts and derived terrestrial impact rates. Icarus 184, 319–326.

Ortner, H.M., Stadermann, F.J., 2009. Degradation of space exposed surfaces by hypervelocity dust bombardment, and refractory materials for space. Int. J. Refractory Met. Hard Mater. 27, 949–956.

Palomba, E., Poppe, T., Colangeli, L., Palumbo, P., Perrin, J.M., Bussoletti, E., Henning, T., 2001. The sticking efficiency of quartz crystals for cosmic sub-micron grain collection. Planet Space Sci 49 (9), 919–926.

Palomba, E., Colangeli, L., Palumbo, P., Rotundi, A., Perrin, J.M., Bussoletti, E., 2002. Performance of micro-balances for dust flux measurement. Adv Space Res 29 (8), 1155–1158.

Piquette, M., Poppe, A.R., Bernardoni, E., Szalay, J.R., James, D., Horányi, M., Stern, S.A., Weaver, H., Spencer, J., Olkin, C., 2019. Student Dust Counter: Status report at 38 AU. Icarus 321, 116–125.

Piquette, M., James, D., Horányi, M., 2020. Calibration of polyvinylidene fluoride based dust detectors in response to varying grain density and incidence angle. Rev Sci Instrum 91. https://doi.org/10.1063/1.5125448 023307.

Pokorny, P., Janches, D., Sarantos, M., Szalay, J.R., Horanyi, M., Nesvorvy, D., Kuchner, M.J., 2019. Meteoroids at the Moon: Orbital Properties, Surface Vaporisation and Impact Ejecta Population. J. Geophys. Res. – Planets 124 (3), 752–778.

Postberg, F. et al., 2014. Stardust Interstellar Preliminary Examination IX: High-speed interstellar dust analog capture in Stardust flight-spare aerogel. Meteorit Planet Sci 49 (9), 1666–1679.

Price, M.C., Kearsley, A.T., Burchell, M.J., Hörz, F., Borg, J., Bridges, J. C., Cole, M.J., Floss, C., Graham, G., Green, S.F., Hoppe, P., Leroux, H., Marhas, K.K., Park, N., Stroud, R., Stadermann, F.J., Wozniakiewicz, P.J., 2010. Comet 81P/Wild 2: The size distribution of finer (sub 10 micrometre) dust collected by the Stardust Spacecraft. Meteorit Planet Sci 45 (9), 1409–1428.

Ratcliff, P.R., Reber, M., Cole, M.J., Murphy, T.W., Tsembelis, K., 1997a. Velocity Thresholds for Impact Plasma Production. Adv Space Res 20 (8), 1471–1476.

Ratcliff, P.R., Burchell, M.J., Cole, M.J., Murphy, T.W., Allahdadi, F., 1997b. Experimental Measurements of Hypervelocity Impact Plasma Yield and Energetics. Int J Impact Eng 20, 663–674.

Rotundi A., et al. Dust measurements in the coma of comet 67P/Churyumov-Gerasimenko inbound to the Sun. Science 347(6220), aaa3905 (6 pages), 2015.

Rudolph, M., Schimmerohn, M., Osterholz, J., Schäfer, E., 2014. Electrical signatures of hypervelocity impact plasma with applications in in-situ particle detection. Acta Astronaut 101, 157–164.

Sauerbrey, G., 1959. Verwendung von Schwingquarzen zur Wägung dünner Schichten und zur Mikrowägung. Zeitschrift für Physik 155 (2), 206–222 (In German).

Schmidt, R.A., 1965. A Survey of Data on Microscopic Extraterrestrial Particles. NASA TN-2719.

Shrine, N.R.G., McDonnell, J.A.M., Burchell, M.J., Gardner, D.J., Holly, H.S., Ratcliff, P.R., Thomson, R., 1997. EuroMir '95: First results from the dustwatch-P detectors of the European space exposure facility. Adv Space Res 20, 1481–1484.

Simon, S.B., Joswiak, D.J., Ishii, H.A., Bradley, J.P., Chi, M., Grossman, L., Aléon, J., Brownlee, D.E., Fallon, S., Hutcheon, I.D., Matrajt, G., McKeegan, K.D., 2008. A refractory inclusion returned by Stardust from comet 81P/Wild 2. Meteorit Planet Sci 43, 1861–1877.

Siraj, A., Loeb, A., 2020. A real-time search for interstellar impacts on the moon. Acta Astronaut 173, 53–55.

Spahn, F., Albers, N., Horning, M., Kempf, S., Krivov, A.V., Makuch, M., et al., 2006. E ring dust sources: Implications from Cassini's dust measurements. Planet Space Sci 54 (9), 1024–1032. https://doi.org/10.1016/j.pss.2006.05.022.

Srama, R., Ahrens, T.J., Altobelli, N., Auer, S., Bradley, J.G., Burton, M., Dikarev, V.V., Economou, T., Fechtig, H., Görlich, M., Grande, M., Graps, A., Grün, E., Havnes, O., Helfert, S., Horanyi, M., Igenbergs, E., Jessberger, E.K., Johnson, T.V., Kempf, S., Krivov, A.V., Krüger, H., Mocker-Ahlreep, A., Moragas-Klostermeyer, G., Lamy, P., Landgraf, M., Linkert, D., Linkert, G., Lura, F., McDonnell, J.A. M., Möhlmann, D., Morfill, G.E., Müller, M., Roy, M., Schäfe, G., Schlotzhauer, G., Schwehm, G.H., Spahn, F., Stübig, M., Svestka, J., Tschernjawski, V., Tuzzolino, A.J., Wäsch, R., Zoo, H.A., 2004. The Cassini Cosmic Dust Analyser. Space Sci Rev 114, 465–518.

Srama, R. et al., 2009. Sample Return of Interstellar Matter (SARIM). Exp. Astron. 23, 303–328.

Stephan, T., 2001. TOF-SIMS in cosmochemistry. Planet. Space Sci. 49, 859–906.

Stansbery, E.K., Draper, D.S., 2014. Role of sample return and sample science in low cost missions. Acta Astronaut 93, 453–459.

Sterken, V.J., Westphal, A.J., Altobelli, N., Malaspina, D., Postberg, F., 2019. Interstellar dust in the solar system. Space Sci Rev 215 (7), 43. https://doi.org/10.1007/s11214-019-0607-9.

Strub, P., Sterken, V.J., Soja, R., Krüger, H., Grün, E., Srama, R., 2019. Heliospheric modulation of the interstellar dust flow on to Earth. A&A 621, A54. https://doi.org/10.1051/0004-6361/201832644.

Szalay, J.R., Horányi, M., 2016. Lunar meteoritic gardening rate derived from in situ LADEE/LDEX measurements. Geophys. Res. Lett. 43, 4893–4898. https://doi.org/10.1002/2016GL069148.

Tabata, M., Imai, E., Yano, H., Hashimoto, H., Kawai, H., Kawaguchi, Y., Kobayashi, K., Mita, H., Okudaira, K., Sasaki, S., Yabuta, H., Yokobora, S.-I., Yamagishi, A., 2014. Design of a silica-aerogel-based cosmic dust collector for the tanpopo mission aboard the international space station. Trans. JSASS Aerospace Tech. Japan 12 (29), 29–34.

Trigo-Rodríguez, J., Domínguez, G., Burchell, M.J., Hörz, F., Lorca, J., 2008. Bulbous tracks arising from hypervelocity capture in aerogel. Meteorit Planet Sci 43, 75–86.

Tsou, P., Brownlee, D.E., Sandford, S.A., Hörz, F., Zolensky, M.E., 2003. Wild 2 and interstellar sample collection and Earth return. J Geophys Res Planets 108, E10, 8113. https://doi.org/10.1029/2003JE002109.

Tuzzolino, A.J., 1995. Applications of PVDF Dust Sensor Systems in Space. Adv. Space Research 17 (12), 123–132.

Tuzzolino, A.J., Economou, T.E., McKibben, R.B., Simpson, J.A., McDonnell, J.A.M., Burchell, M.J., Vaughan, B.A.M., Tsou, P., Hanner, M.S., Clark, B.C., Brownlee, D.E., 2003. Dust Flux Monitor Instrument for the Stardust Mission to Comet Wild 2. J. Geophys. Res **E** 108 (E10), 8115. https://doi.org/10.1029/2003JE002086.

Tuzzolino, A.J., Economou, T.E., Clark, B.C., Tsou, P., Brownlee, D.E., Green, S.F., McDonnell, J.A.M., McBride, N., Colwell, M.T.S.H., 2004. Dust Measurements in the Coma of Comet 81P/Wild 2 by the Dust Flux Monitor Instrument. Science 304 (5678), 1776–1780.

Vaverka, J., Pavlu, J., Nouzá, L. k., Safrankova, J., Nemecek, Z., Mann, I. B., Ye S., Lindqvist P.-A. One-year analysis of dust impact-like events onto the MMS spacecraft. Journal of Geophysical Research: Space Physics 124, 8179 – 8190 (2019).

Westphal A.J., Flynn G.J., Sutton S.R., Bunch T., Borg J., Bibring J.-P. and Chadin A. Identification and Chemical Composition of Particles Captured in Aerogel Flown on the MIR Space Station. 29th Annual Lunar and Planetary Science Conference, abstract no. 1917 (1998).

Westphal, A.J., Snead, C., Butterworth, A., Graham, G.A., Bradley, J.P., Bajt, S., Grant, P.G., Bench, G., Brennan, S., Pianetta, P., 2004. Aerogel keystones: Extraction of complete hypervelocity impact events from aerogel collectors. Meteorit Planet Sci 39, 1375–1386.

Westphal, A.J., Fakra, S.C., Gainsforth, Z., Marcus, M.A., Ogliore, R.C., Butterworth, A.L., 2009. Mixing fraction of inner solar system material in Comet 81P/Wild 2. The Astronomical Journal 694, 18–28.

Westphal, A.J. et al., 2014. Evidence for Interstellar Origin for Seven Dust Particles Collected by the Stardust Spacecraft. Science 345 (6198), 786–791.

Whipple, E.C., 1981. Potentials of Surfaces in Space. Rep Prog Phys 44, 1197–1250.

Whitely R., and Martinez R., Options for Staging Orbits in Cislunar Space. 2016 IEEE Aerospace Conference. IEEE Aerospace Conference Proceedings, 9pp. (2016). DOI: 10.1109/AERO.2016.7500635.

Woignier T., Duffours L., Colombel P., and Durin C. Advances in Materials Science and Engineering vol. 2013, Article ID 484153, 6 pages (2013). http://dx.doi.org/10.1155/2013/484153.

Wozniakiewicz, P.J., Kearsley, A.T., Ishii, H.A., Burchell, M.J., Bradley, J.P., Teslich, N., Cole, M.J., Price, M.C., 2012a. The Origin of Crystalline Residues in Stardust Al Foils: Surviving Cometary Dust or Crystallized impact Melts? Meteorit Planet Sci 47, 660–670.

Wozniakiewicz, P.J., Ishii, H.A., Kearsley, A.T., Burchell, M.J., Bradley, J.P., Price, M.C., Teslich, N., Lee, M.R., Cole, M.J., 2012b. Stardust Impact Analogues: Resolving Pre- and Post-Impact Mineralogy in Stardust Al Foils. Meteorit Planet Sci 47, 708–728.

Wozniakiewicz P.J., Bradley J.P. Ishii H.A., Brownlee D.E. Price M.C. Pre-Accretional Sorting of Grains in the Outer Solar Nebula. The Astrophysical Journal 779:164 (6pp), 2013.

Wozniakiewicz, Penelope J., Burchell, Mark J., 2019. Space Dust and Debris Near the Earth. Astron Geophys 60 (3), 38–42. https://doi.org/10.1093/astrogeo/atz150.

Wozniakiewicz, P.J., Kearsley, A.T., Bridges, J., Holt, J., Price, M.C., Burchell, M.J., Hicks, L., 2019. Orbital Dust Impact Experiment (ODIE) – A passive dust collector designed to address the dust flux data gap. In *Proceedings of the 1st International Orbital Debris Conference*, Abstract 6149.

Yano, H., Collier, I., Shrine, N., McDonnell, J.A.M., 1996. Microscopic and Chemical Analyses of Major Impact Sites on Timeband Capture Cell Experiment of the EuReCa Spacecraft. Adv. Space Res. 17 (12), 189–192.

Zhang, C., Feng, G., Sui, S., 1997. Study of behaviour of QCM sensor in loading variation. Sensors and Actuators B40, 111–115.

Zolensky, M., Pieters, C., Clark, C., Papike, J.J., 2000. Small is beautiful: The analysis of nanogram-sized astromaterials. Meteorit Planet Sci 35, 9–29.

Zubarev, R.A., Makarov, A., 2013. Orbitrap Mass Spectrometry. Anal Chem 85, 5288–5296.